Nuclear Engineering and Design 335 (2018) 356–373

Contents lists available at ScienceDirect

Nuclear Engineering and Design

journal homepage: www.elsevier.com/locate/nucengdes

The upgraded Cheng and Todreas correlation for pressure drop in hexagonal wire-wrapped rod bundles

S.K. Chen[a,*,1], Y.M. Chen[a], N.E. Todreas[b]

[a] Institute of Nuclear Engineering and Science, National Tsing-Hua University, Hsinchu 30013, Taiwan
[b] Department of Nuclear Science and Engineering, Massachusetts Institute of Technology, Cambridge, MA 02139, USA

ARTICLE INFO

Keywords:
Wire-wrapped
Pressure drop
Friction factor
Correlation

ABSTRACT

The Cheng and Todreas (detailed) correlation (CTD) for wire-wrapped rod bundle friction factor published in 1986 has been identified in Chen et al. (2014) as the most used correlation for design and safety analyses for the Generation IV Sodium Fast Reactor(SFR). Since its publication in 1986, sixteen additional wire wrapped fuel bundle experiments have been performed worldwide providing data to supplement regions of minimal data in the bundle test data base. Based on this valuable new data, the CTD correlation has been refined in the following three aspects and renamed the Upgraded CTD (UCTD) Correlation.

1. The laminar to transition boundary Reynolds value has been significantly reduced. As well, a new laminar boundary equation is adopted which gives much lower value for the laminar boundary (Re_{bL}) as a function of P/D.
2. The transition region equation for bundle friction factor modified by Chen et al. (2013) to make the friction factor trajectory smoother moving through the turbulent boundary now has the exponent λ reassessed to the value of 7.
3. The UCTD is now applicable to 7-pin bundle geometry. This has been achieved by adjusting the bundle average friction factor predicted by CTD for most bundle geometries such that the bundle fiction factor increases as the pin number increases. The cause of the previous inverse behavior was identified as the formulation of the wire drag and wire swirl empirical constants. A new process for finding these empirical constants is proposed and the constants set is calibrated by an 80 bundle data set. For Rehme's set of twenty 7 pin bundle experiments, the mean error prediction is now 9% which is about the measurement uncertainty and improved from 26% with CTD.

The new correlation incorporating the above three improvements to the original CTD correlation is designated as the Upgraded CTD (UCTD) correlation. For the available 118 wire-wrapped bundles with pin number greater than 7 bundles, UCTD predicts the data in the transition and turbulent regimes with a mean error of 0.95% and a 90% confidence interval of ± 14.8%, while both the CTD and the Rehme correlations (REH) have 1.5% higher values of this index. For the 27 available bundles with laminar data,(none of which are as small as 7 pin bundles) the performance of UCTD is slightly better than CTD with mean and RMS values of −2.0%, and 9.5% versus −3.0%, and 9.6%. (The REH correlation is not applicable to the laminar regime).

A web-based numerical code of the UCTD correlation which incorporates these advances has been provided on the web for convenient design and research use.

1. Introduction

1.1. Purpose of this paper

The purpose of the paper is to provide enhancements for both design and research application of the existing Cheng and Todreas (CT) correlation. The experimental confirmation of these correlation enhancements has been made possible by the sixteen additional wire -wrapped rod bundle experiments reported since the publication of our original bundle pressure drop correlation which are summarized in Section 1.3 Literature review below. For design application the correlation updates include redefinition of the laminar to transition

* Corresponding author at: 101, Section 2, Kuang-Fu Road, LTM Building Room 111, Hsinchu 30013, Taiwan.
E-mail address: shihkueichen@gapp.nthu.edu.tw (S.K. Chen).
[1] Formally legally known as S.K. Cheng.

https://doi.org/10.1016/j.nucengdes.2018.05.010
Received 14 February 2018; Received in revised form 3 May 2018; Accepted 7 May 2018

Nomenclature

A	Axial average flow area
A_r	Projected area of wire in a subchannel
C_f	Friction factor constant defined in Eqs. (A1) and (A2)
D	Rod diameter
De	Equivalent hydraulic diameter
D_w	Wire diameter
f	Darcy friction factor, if no subscript means bundle average value
H	Wire lead length
L	Axial Length
N	Number of each kind of subchannel in the bundle
Nr	Number of pins in the bundle
P	Rod pitch
ΔP	Pressure drop
P_w	Wetted perimeter
Re	Reynolds number (=ρVDe/μ), if no subscript means bundle average value
Re_{bL}	Laminar to transition boundary Reynolds number
Re_{bT}	Transition to turbulent boundary Reynolds number
V	Axial velocity
W	Edge pitch parameter defined as (D + gap between rod and bundle wall)
W_d	Wire drag constant
W_s	Wire swirl constant
X	Flow split parameter for each subchannel defined as (V_i/V_b)
ρ	Coolant density
μ	Dynamic viscosity
θ	Angle which the wire makes with respect to vertical axis
Ψ	Intermittency factor
m	Mean value of the normal distribution
σ	Standard deviation of the normal distribution
λ	Exponent used in revised transition friction factor formulae

Subscript

i	1, 2, 3 or b denote interior, edge, corner subchannel type, or bundle average, respectively
f	Denotes friction
L	Denotes laminar flow region
T	Denotes turbulent flow region
tr	Denotes transition flow region

Superscript

‘	Denotes equivalent bare rod values (without considering wire)

boundary, updated formulae for the friction factor in the transition regime and reformulation of fitted constants for wire drag (W_d) and wire swirl (W_s) to more correctly predict the effect of bundle pin number variation. For research application the applicable range of the CTD correlation is extended to the seven pin bundle geometry. Importantly the trend of friction factor with pin number has been focused upon to yield the correct trend of friction factor increase with increasing number of pins albeit at a decreasing rate. The strategy and structure of the original correlation is summarized next in Section 1.2 to provide the context for the proposed enhancements.

1.2. The existing Cheng and Todreas correlation for wire wrapped bundle pressure drop

The Cheng and Todreas correlation (CT) for hexagonal wire-wrapped rod bundle pressure drop was published in 1986. The correlation was based on the development of friction factors for the three types of hexagonal bundle subchannels; namely, interior, edge and corner subchannels, as illustrated in Fig. 1. The bundle average friction factor is predicted by subchannel friction factors based upon the fact that pressure drops are the same for different subchannel, i.e., neglecting entrance, exits and momentum losses. It has been enhanced by Chen et al. (2013) by modification of the transition region correlation in the immediate vicinity of the transition to turbulent region boundary and validated in 2014 (Chen et al., 2014) as the superior correlation available in the literature for bundle geometries of both design and research interest.

The experimental data of bundle average friction factor are determined by the measured pressure drop over a length L in a wire-wrapped rod bundle.[2] These experimental data clearly show that there are three flow regimes for this parameter. Below a specific bundle Reynolds number the friction factor is proportional to $1/Re_b$, hence, the laminar regime. As the Re_b increases the flow enters the transition regime, and finally at a sufficiently high Reynolds number the flow becomes fully turbulent. These two transition Reynolds numbers Re_{bL} and Re_{bT} are two cornerstones of the CT correlation.

The bundle average friction factor constant, C_{fbT} and C_{fbL} for the turbulent flow regime and the laminar flow regime, respectively, are determined by $C_{fb} = f_b \times Re_b^m$ with m = 0.18 for the turbulent regime and m = 1 for the laminar regime. These bundle average friction factor constants are functions of geometrical parameters and subchannel friction factor constants C_{fiT} or C_{fiL}, which contain the empirical constants W_d and W_s, formulated to reflect the specific effect of the wire wrapping as described below.

The enhancement of the wire-wrapped subchannel friction factors relative to the bare rod values are caused by two hydrodynamic mechanisms. For the interior subchannel, the pressure loss due to wire drag was evaluated by a theoretical drag loss characterized by an empirical constant, W_d (wire drag constant). The other pressure loss enhancing mechanism effect is a swirl flow induced by the wire, creating a tangential flow which increases the flow path in the edge and corner subchannels, hence the pressure loss, and the friction factor for these subchanneis. The empirical constant W_s (swirl flow constant) was used to reflect the actual value of this effect. These two constants are geometrical parameters as well as flow regime dependent, and must be

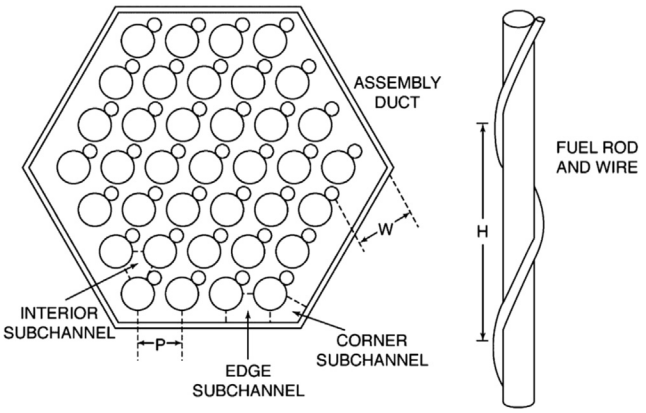

Fig. 1. Typical sodium cooled fast reactor (SFR) wire-wrapped assembly and rod configuration.

[2] Bundle axially average friction factor $f_b = \Delta P(De_b/L)(2/(\rho V_b^2))$. The pressure at each axial plane is that averaged across the bundle cross section.

Table 1
New wire-wrapped rod bundle pressure drop experiments since year 2016.

Identification Designation	Reference	Coolant	Pin number	D (mm)	D_w (mm)	P/D	W/D	H/D	Range of Re_b
PGSFR1	Korea – Chang et al. (2016)	water	37	7.40	0.93	1.125	1.125	27.69	4300–40,000
PGSFR2	Korea – Chang et al. (2017)	water	61	8.00	1.00	1.125	1.125	29.86	13,000–60,000
PFBR	India – Padmakumar et al. (2017)	water	217	6.60	1.65	1.255	1.255	30.30	200–52,000
JSFR 1	Japan – Ohshima and Imai, (2017)	water	127	5.50	0.90	1.176	1.176	38.00	200–70,000
JSFR 2			169	6.50	1.32	1.211	1.211	47.23	230–83,000
JSFR 3			271	7.50	1.40	1.200	1.200	22.00	490–58,000
THEADES	Europe (KIT – Germany) – Pacio et al. (2016)	LBE*	19	8.20	2.20	1.279	1.290	40.00	14,000–48000
COMPLOT	Europe (SCK-CEN-Belgium) – Pacio et al. (2017)	LBE	127	6.55	1.80	1.279	1.290	40.00	4000–32,000
TAMU	United States (Texas A&M) – Veghetto et al. (2018)[a]	p-Cymene	61	15.9	3.0	1.189	1.231	30.00	260–19,000

* LBE = Liquid Bismuth Eutectic.

[a] The new data were measured using regular rod in stead of extremely smooth acrylic rod and wire used originally, and the data were provided by Professor Hassan (2018).

calibrated by the related data in a cautious way to get the correct results and sound trend with increasing bundle size (pin number) of the bundle average friction factors. Since most experiments have turbulent regime data, the calibration of the two constants designated as W_{dT} and W_{sT} was initiated from the turbulent regime.

For the laminar regime, since only 19 laminar bundle friction factor results were available at the time CTD was developed, they are insufficient to meaningfully calibrate the constants as functions of P/D and/or H/D. Instead, by some theoretically arguments and assumptions, these constants in the laminar regime were established as proportional to turbulent.

Two versions of the CT correlation have existed – the detailed formulation (CTD) and a simplified version (CTS). The correlation has now been made available online for easy user access.[3] With the existence of this online version the need for the CTS version for simplified manual calculation has been superseded so that further upgrade of CTS has been terminated. This paper proposes an enhanced version of the existing CTD correlation named the Upgraded Cheng and Todreas Detailed Correlation (UCTD) which includes the enhanced capabilities identified above. The full form of the UCTD recommended in this paper is presented in Appendix A.

1.3. Literature review

Effort on development of predictive capabilities for assessing hexagonal wire-wrapped rod bundle pressure drop has been ongoing since the 1970s to support the deployment of the early sodium cooled fast reactors. In the last decade interest in Gen IV sodium fast reactors and the Belgium MYRRHA lead-bismuth alloy cooled subcritical reactor has generated renewed activity in this area. Hence it is instructive to consider correlation developments and most importantly correlation assessment activities based upon the multitude of experimental bundle pressure drop experiments in their approximate chronological publication sequence.

Up to 1986, there were about ten correlations developed for wire-wrapped rod bundle pressure drop prediction, including Novendstern (1972) (NOV), Rehme (1973) (REH), Baxi and Dalle Donne (1981) (BDD), the detailed and simplified Cheng and Todreas (1986) (CTD and CTS), and some Russian correlations, represented as Kirillov et al. (2010) (KIR). Several investigators (Chun and Seo (2001), Bubelis and Schikorr (2008), Chen et al. (2014)) have performed evaluations for assessing the predictive performance of these correlations for wire-wrapped rod bundle friction factors. The most thorough study was performed by Chen et al. (2014), who assessed the most appropriate data base utilizing several comparison parameters to assess the best fit correlation for ten evaluation cases. This assessment found that of the ten evaluation cases, nine identified the best fit correlation as CTD. The exception was the 108 bundle set case covering the transition and turbulent regimes, in which half of the 108 bundles are Rehme bundles on which Rehme performed measurements.

At the time the CTD was developed, the available pressure drop experiments using wire-wrapped rod bundles were collected and documented by Cheng (1984). At that time, there were totally 125 experiments, of which 74 bundles were performed by Rehme (1967) and 51 bundles by the other investigators. Of these 51 bundles, two of them apply for H/D > 52 geometry, and one applies for H/D = 4 (hence both are out of the general application range of $8 \leqq H/D \leqq 52$). Hence these three bundles were excluded from the data base for assessing correlations. From 1984 to 2013, seven new experiments were performed, five in Korea Chun and Seo (2001) and Choi et al. (2003) and two in Europe, ESTHAIR Berthoux and Cadiou (2010) and ISPRA Chenu et al. (2011). In total, the bundle number became 129 (125 − 3 + 7). To reduce the possible systematic error by the same investigator, only one bundle with the highest pin number for each geometrical set of Rehme's experiments, hence only 25 Rehme bundles, were included in the assessing data base. This strategy results in 80 bundles (51 − 3 + 7 + 25) for the assessing the data base.

Since 2016 nine additional wire-wrapped rod bundle experiments have been performed in Korea (2 experiments of 37 and 61 pins), India (1 experiment of 217 pins), Japan (3 experiments of 127, 169 and 217 pins), Europe (1 experiment of 19 pins and 1 full scale MYRRHA 127 pin bundle) and United States (1 experiment of 61 pin) to validate and verify the design tools and/or correlations. Table 1 specifies the bundle characteristics including dimensions of these new experiments. Most of the results fit the CTD closely as stated by the investigators themselves, except for the Europe COMPLOT experiment as well as the earlier performed 2010 ESTHAIR experiment (Berthoux and Cadiou, 2010) for which the predictions of the Rehme correlation better fit the data than did the CTD correlation.

To design a reactor core or perform safety analysis, subchannel analysis is essential. Most subchannel analysis codes now being used to perform these wire wrapped bundle designs use the CTD correlation, including CADET and TRIO-U (France – Tenchine, 2010; Conti et al., 2017), MATRA-LMR (Korea – Kim et al., 2002) and SE2-ANL (USA-Yang and Yacout, 1995). Recently developed subchannel codes for general analysis purposes include the ANTEO+ code (Lodi et al., 2016), the Assembly Design and OPTimization (ADOPT) code (Qvist and Greenspan, 2016) and the SAM (System Analysis Module) theory developed at Argonne National Lab (Hu, 2017).

ANTEO+ uses the Rehme correlation as the default rod friction factor equation with CTD as optional. The other two, ADOPT and SAM use the CTD for their bundle friction factor calculation.

Based on the studies above, the CTD has been identified to be the best fit wire-wrapped rod bundle friction factor correlation, not only because of its prediction accuracy, but also because of its application

[3] A code for calculation of the Upgraded Cheng-Todreas correlations can be found at the following site: http://wp.me/p61TQ-tI.

range covers all flow regimes, the widest range of P/D (1.0–1.42) and H/D (4–52) as well as the capability of reducing to the bare rod bundle result as the wire diameter goes to zero. The later capability is due to the fact that the correlation was constructed by adding the wire effect to the bare rod results, which was fitted from Rehme's G*-method (Rehme, 1973). However, the pin number of the bundle must be larger than or equal to 19; the CTD is not valid for 7-pin bundles.

It is now most commonly used for determination of subchannel friction factor values in subchannel analysis codes used to calculate the temperature distribution in a fuel bundle. However, our experience has indicated that the Cheng and Todreas correlation can be further improved in several specific regards. These enhancements are identified and developed in the following sections.

2. The aspects of the Cheng and Todreas correlation that merit improvement

2.1. Revision of the designated Reynolds number value for the laminar to transition boundary

As described in Section 1.2 for a wire-wrapped rod bundle, there is a Re_{bL} below which the flow is in the laminar regime. The comparisons between data in the transition regime near the laminar-transition boundary and predictions of CTD show that a lower designated Reynolds number (around Re_{bL} = 400) than originally specified for the laminar-transition boundary gives dramatic improvement of predictions near the laminar-transition boundary. For example the high P/D (=1.42) bundle data demonstrates the Re_{bL}(=1550) is too high to well predict the trend of the data in transition region, as shown in Fig. 2 for the Rehme51c bundle. The prediction by CTD can be improved dramatically if Re_{bL} is decreased to a much lower value.

Since there were no data available in 1986 for P/D > 1.256 (note that this situation still exists now), the original Re_{bL} equation was calibrated using data from wire wrapped bundles with P/D < 1.256 and Rehme's bare rod bundle data with P/D > 1.25. During the last three decades more wire-wrapped bundle tests have been performed to secure laminar data so that redefinition of the laminar to transition boundary is possible to allow the correlation to give lower values for the Re_{bL} value at this boundary without using Rehme's bare rod results.

2.2. New formula for the friction factor in the transition regime

A revised transition formula has been proposed and published in Chen et al. (2013). This revision was made by addition of a constant parameter λ to correct for a sudden decrease in friction factor in the vicinity of the turbulent boundary which thus avoided the occurrence of a reversal in pressure drop as the flow rate increases. The issue is whether the constant parameter λ value in the revised formula is the optimum value since the bundle data base is now larger than was available for use when the 2013 paper was written. A revised value needs to be determined.

2.3. Correct pin number effect

The bundle friction factor predicted by CTD decreases slightly as the pin number increases in the bundle P/D geometrical range 1.08 < P/D < 1.38 for H/D = 25. However, Rehme's experimental results and computational fluid dynamics (CFD) calculation show that friction factor increases as pin number increases (Rolfo et al., 2012). Since the effect is minor this characteristics does not affect the accuracy of CTD. But since CTD is based on a theoretical combination of subchannel friction factors to predict the bundle friction factor, why does it predict this opposite trend ? To make the correlation sound, the reason for this behavior needs to be explained and the needed revision of the CTD to predict the correct pin number effect should be made.

2.4. Extend the capability to include predicting 7-pin bundles

The current application range for CTD does not include 7-pin bundles. Due to the incorrect prediction of the trend of the pin number effect, the CTD normally over predicts 19-pin bundle data by about 5–10%, and 7-pin bundles by about 20–30%. It is desirable to revise the CTD so that it is capable of prediction of pressure drop behavior of 7 pin bundles. Additionally if the pin number effect of Section 2.3 above can be corrected, it might automatically extend the application of CTD to 7-pin bundles.

3. Proposed improvements to the CTD correlation

3.1. Revised laminar to transition boundary

The laminar to transition boundary (Re_{bL}) and transition to turbulent boundary (Re_{bT}) for the existing CT correlation were calibrated as Cheng and Todreas (1986),

$$\log\left(\frac{Re_{bL}}{300}\right) = 1.7\left(\frac{P}{D}-1.0\right) \quad (1)$$

$$\log\left(\frac{Re_{bT}}{10{,}000}\right) = 0.7\left(\frac{P}{D}-1.0\right) \quad (2)$$

Reexamining the friction factor data for bundles that have laminar regime data shows that the laminar boundary should be much lower than the values calculated by Eq. (1). The comparisons between data in the transition regime near the laminar boundary and predictions of CTD show that selection of a lower laminar boundary value (around Re_{bL} = 400) gives dramatic improvement of predictions near the laminar boundary. Estimating the Re_{bL} by visual inspection of friction factor data, the least squares regression of these data yields the following equation,

$$\log\left(\frac{Re_{bL}}{320}\right) = \left(\frac{P}{D}-1.0\right) \quad (3)$$

The bundle data and proposed Re_{bL} as function of (P/D) are shown in Fig. 3.

In Fig. 4 the 19-pin and 37-pin data for the Rehme53 bundle are presented together with the correlation predictions with different Re_{bL}. It is clear that with the current laminar to transition boundary of Re_{bL} = 1550, the prediction is far from satisfactory. However, Fig. 4 shows the improvement of the fit to data if the new Re_{bL} of 800 consistent with Eq. (3) is used. Note the correlation matches the 19-pin and 37-pin data fairly well and the data for 37-pin bundle are always higher than that of 19-pin bundle.

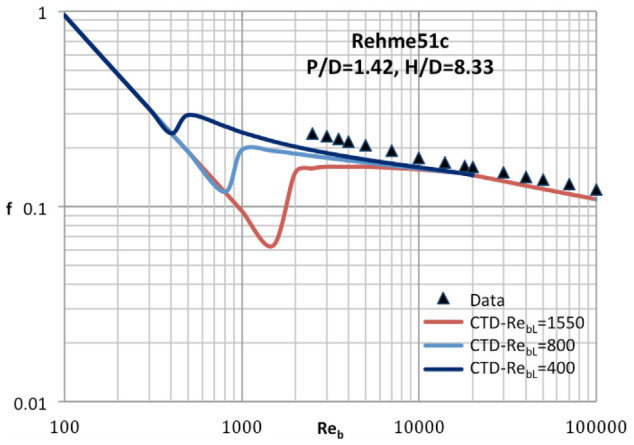

Fig. 2. Comparison between data and prediction of CTD with different Re_{bL} values for the Rehme51c bundle.

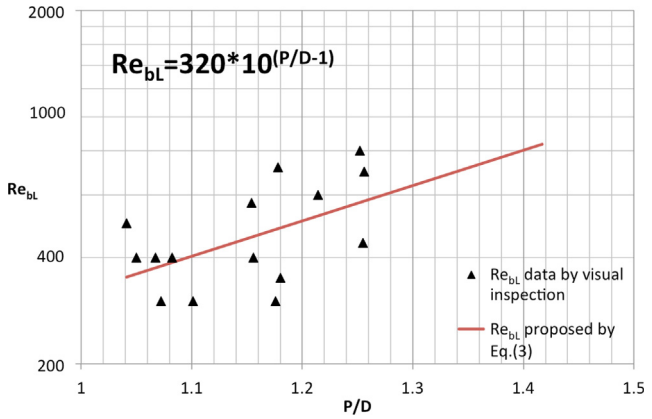

Fig. 3. Revised laminar to transition boundary Re_{bL} as a function of P/D.

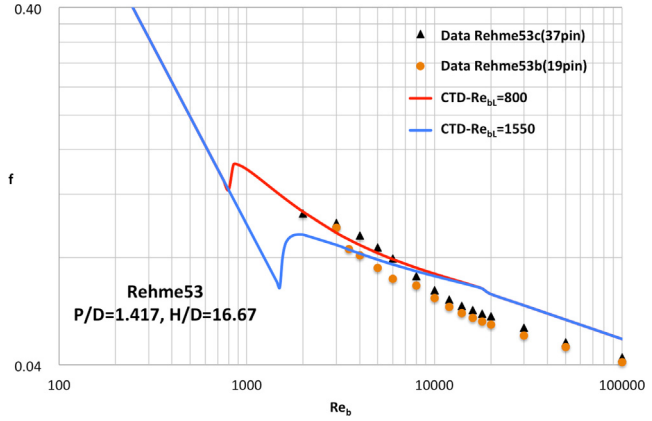

Fig. 4. Comparison between data and CTD friction factor predictions for different Re_{bL} values for the Rehme53 bundle.

3.2. Formulae for friction factor in the transition regime

The transition regime formula has been modified and published in Chen et al. (2013). The new equation is in the form as

$$f_{btr} = f_{bL}(1-\psi_b)^{1/3}(1-\psi_b^{\lambda}) + f_{bT}\cdot\psi_b^{1/3} \tag{4}$$

where

$$\psi_b \equiv \log\left(\frac{Re_b}{Re_{bL}}\right)/\log\left(\frac{Re_{bT}}{Re_{bL}}\right) \tag{5}$$

The constant λ was calibrated as 13 when 58 bundles of transition data were used. Although the main purpose of this new 2013 equation was to eliminate the reverse pressure calculated as flow increases near the transition to the turbulent boundary, as long as its value is between 3 and 30, there would be a negligible effect on the resulting friction factor. The objective of this currently proposed modification is to make the friction factor curve as smooth as possible at the transition to turbulent boundary as the data indicate.

Recalibration of this constant has been performed using data in the transition regime of the 80-bundles data set yielding the performance index results shown in Table 2. The main index for identifying the goodness of fit of each correlation is the 90% confidence interval (C.I.), which means that 90% of the data base will lie inside the specified ± xx % interval. For a normal distribution, this interval is easily determined by the mean and standard deviation (STD). Table 2 shows the three major indices for prediction error using different values of λ. Fig. 5 shows the friction factor behavior for various λ values near the transition to turbulent boundary for the Chun1 bundle (Chun and Seo, 2001). The λ = 7 value is selected since the predicted curve for transition to the turbulent region is smoother than others, as illustrated in Fig. 5, and its 90% confidence interval is the lowest as shown in Table 2.[4]

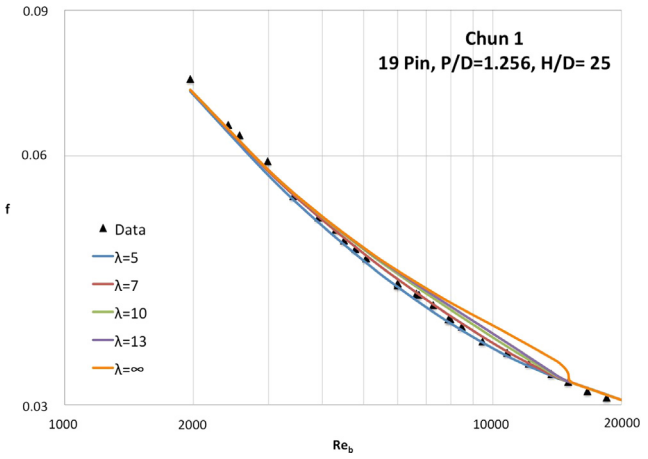

Fig. 5. Comparison the smooth transition to turbulent of transition friction factor behavior with data for different λ.

3.3. Pin number effect issue and correction—revision of empirical constants

3.3.1. Trend of bundle friction factor as pin number increases

Rehme (1967) performed a series of wire-wrapped rod bundle pressure drop experiments with five P/D (1.125; 1.233; 1.275; 1.343 and 1.417) and five H/D (8.33; 12.5; 16.67; 25 and 50), a total of 25 sets of bundle geometrical parameters. For each of the geometrical sets, there are three bundles containing different numbers of pins. These experiments show a general trend that the bundle average friction factor increases as pin number increases. This is consistent with the fact that for larger bundles, the friction losses are higher because the bypass effect at the edges becomes less dominant. Fig. 6 compares the friction factor constants among the data and predictions of CTD and REH for 19- and 37-pin bundles with H/D = 16.67; the data for P/D < 1.1 were performed by Marten et al. (1982). The percentage increase from 19 pin to 37 pin bundles is around 5–10%. For pin number higher than 37, the increase amount is much smaller, generally less than 3%. CFD calculations by Rolfo et al. (2012) also confirm the increase of bundle friction factor as pin number increases; however, the increase is insignificant compared to the data uncertainty.

Although CTD was demonstrated to be the best correlation for predicting wire wrapped bundle pressure drop, it does not predict the correct trend as pin number increases, as shown in Fig. 6. Note that the Rehme correlation uses a simple correction factor (total rod wetted perimeter divided by bundle wetted perimeter) to account for the pin number effect. Fig. 6 illustrates that the CTD for 19 pins (CTD-19) predicts a value higher than REH-19 by 20%. Since Rehme's correlation predicts his own data within 5% error, one could expect that CTD over predicts Rehme's 19 pin bundles by more than 15%. Since our data base predominantly includes bundles with pin number higher than 19, this effect does not influence the accuracy of CTD pressure drop predictions even though CTD predicts a reverse trend as pin number increases for most pin bundle geometries.

3.3.2. The cause of the reverse trend in CTD predictions as pin number increases

The CTD subchannel friction factor formulae, include a constant

[4] Here and in later Tables where multiple indices of correlation predictions are presented, we preferentially base necessary parameter selections on the 90% confidence interval index since it inherently also reflects the behavior of the Mean Error and the STD indices.

Table 2
Indices for goodness of correlation predictions for the transition regime of all 80 bundles.[a]

Index\ λ	3	5	7	10	13	∞
Mean Error	−3.6%	−1.3%	−0.32%	−0.43%	−0.81%	1.68%
STD of Error	9.37%	9.38%	9.45%	9.54%	9.62%	9.80%
90% C. I.	± 16.52%	± 15.59%	± 15.56%	± 15.72%	± 15.87%	± 16.36%

[a] For statistical analysis see Larsen and Marx (2012).

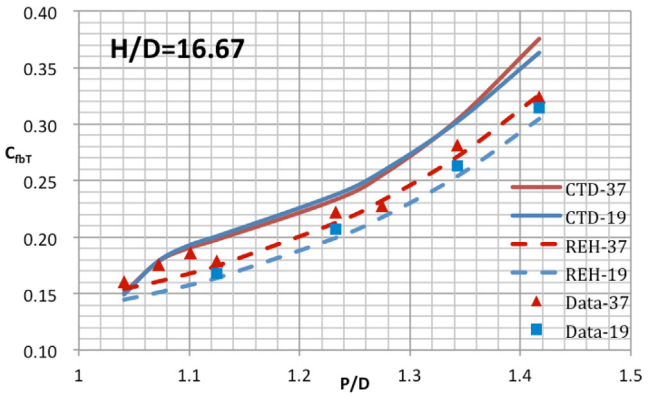

Fig. 6. Comparison among predictions and data for turbulent friction factor constants (C_{fbT}) of 19- and 37-pin bundles with H/D = 16.67.

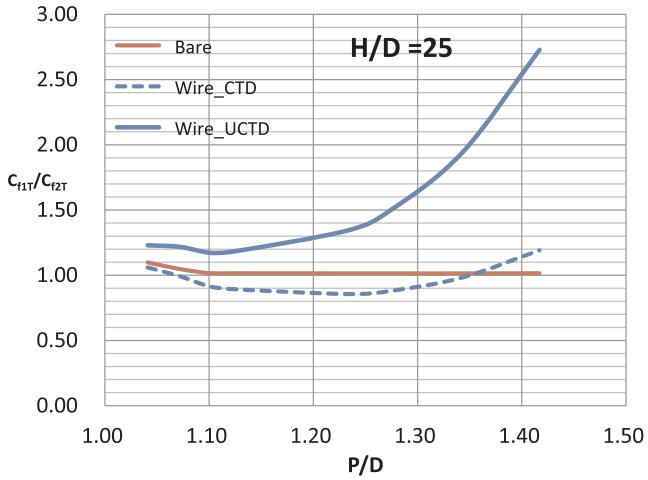

Fig. 7. Ratio of interior subchannel friction factor constant to that of edge subchannel in the turbulent regime for wire-wrapped and bare rod bundle predicted by the CTD and UCTD with H/D = 25.

related to drag force (W_d) for interior subchannels, and a constant related to the swirl flow (W_s) for edge and corner subchannels. Specifically for the turbulent regime, the formulae for the subchannel friction factor constants for the three types of subchannel are (subscript 1 for interior, 2 for edge, 3 for corner),

$$C_{f1T} = C'_{f1T}\left(\frac{P'_{w1}}{P_{w1}}\right) + W_{dT}\left(\frac{3A_{r1}}{A'_1}\right)\left(\frac{De_1}{H}\right)\left(\frac{De_1}{D_w}\right)^{0.18} \quad (6)$$

$$C_{f2T} = C'_{f2T}\left(1 + W_{sT}\left(\frac{A_{r2}}{A'_2}\right)\tan^2\theta\right)^{1.41} \quad (7)$$

$$C_{f3T} = C'_{f3T}\left(1 + W_{sT}\left(\frac{A_{r3}}{A'_3}\right)\tan^2\theta\right)^{1.41} \quad (8)$$

In the turbulent regime these two empirical constants (i.e., W_{dT} and W_{sT}) were optimally calibrated through an iterative process (Cheng, 1984), using all pin bundle average friction factor constants and flow split data available in 1984, except 7 pin results. The resulting constant set are shown below.

$$W_{sT} = 20.0\log\left(\frac{H}{D}\right) - 7.0 \quad (9)$$

$$W_{dT} = \left(29.5 - 140\left(\frac{D_w}{D}\right) + 401\left(\frac{D_w}{D}\right)^2\right)\left(\frac{H}{D}\right)^{-0.85} \quad (10)$$

For a hexagonal bundle, the number of corner subchannels is always 6, and the number of edge subchannels increases much slower than interior subchannels as pin number increases. The bundle average friction factor thus increases as the pin number increases, since the friction factor for an interior subchannel is higher than that of an edge subchannel. However, if these relative friction factor values are reversed, then the bundle average values will decrease as pin number increases.

For bare rod bundles, this increasing trend was observed. The interior subchannel friction factor calculated from CTD with wire diameter equal to zero is higher than that of edge subchannel. The bare rod bundle experimental results performed by Rehme (1972) did show that this bundle friction factor constant increases as pin number increases.

However for wire wrapped bundles, depending on the W_s and W_d values assigned in Eqs. (6)–(8), the calculated interior subchannel friction factor constant is not necessarily higher than that of the edge subchannel. The set of W_{dT} and W_{sT} (Eqs. (9) and (10)) in CTD unfortunately do not avoid this condition over a large portion of the H/D and P/D geometrical range. The W_{sT} increases as H/D increases, while W_{dT} is inversely proportional to H/D. This situation enhances this reverse pin number effect. Investigation showed that for CTD this reverse trend becomes worst when H/D = 50 and P/D is around 1.2. This undesirable behavior of the CTD is illustrated in Fig. 7 for the ratio of interior subchannel turbulent friction factor constant divided by that of edge subchannel (i.e., C_{f1T}/C_{f2T}) for H/D = 25 over a range of P/D values. As well for comparison purposes Fig. 7 also shows that proper behavior is obtained for CTD applied to bare rod bundles and for the upgraded CTD (UCTD) correlation proposed later in this paper when applied to wire wrapped pins.

3.3.3. *Selection of empirical constants W_{sT} and W_{dT} in the turbulent regime to obtain the correct pin number trend*

The proposed selection of the empirical constants W_{sT} and W_{dT} is designed to achieve the following goals. 1) predict the correct pin number trend, 2) predict the friction factor data as well as the current CTD correlation constants do so and 3) predict the flow split consistent with data. The approach is to first find the turbulent coefficients W_{sT} and W_{dT} based on the chosen sufficient and appropriate 80-bundle data base, and then to establish the corresponding laminar parameters W_{sL} and W_{dL} as simply equal to each of the turbulent parameters times an individual multiplying factor.

The process is focused on determining the factors a,b which define the parameter W_{sT} in the following equation which follows the format of Eq. (9),

$$W_{sT} = W_{sT}(a,b) = a\cdot\log\left(\frac{H}{D}\right) + b \tag{11}$$

and then establish W_{dT} from the C_{fbT} value calculated from the 80-bundle data set (note that one of these bundles did not have turbulent data) by solving the following equation,

$$C_{fbT} = De_b\left(\sum_{i=1}^{3}\left(\frac{N_iA_i}{A_b}\right)\left(\frac{De_i}{De_b}\right)^{0.0989}\left(\frac{De_i}{C_{fiT}}\right)^{0.54945}\right)^{-1.82} \tag{12}$$

in which C_{f2T} and C_{f3T} are functions of W_{sT}, and C_{f1T} contains W_{dT}. The 79 W_{dT} values which are obtained in this manner are fitted by the following form of Eq. (13) as in the original CTD, i.e.

$$W_{dT} = \left(C_1 + C_2\left(\frac{D_w}{D}\right) + C_3\left(\frac{D_w}{D}\right)^2\right)\left(\frac{H}{D}\right)^{C_4} \tag{13}$$

The process for determination of the needed empirical constants W_{sT} and W_{dT} in the turbulent regime is presented in Appendix B. which identifies seven candidate W_{sT} [(-8,17), (-9,18), (-10,18), (-10,19), (-11,19), (-11,20) and (-12,21)] and associated W_{dT} sets.

While each of these sets fulfills our objectives of yielding the satisfactory pin number effect trend, similar if not better pressure drop prediction than CTD and percent error within the flow split measurement uncertainty of 10%. To distinguish which set we should adopt for the upgraded CTD (UCTD), we next study their relative capabilities in predicting the turbulent regime data. Table 3 shows goodness of fit in the turbulent regime for these seven sets of constants as well as the original CTD. The pin number effect is correct for all seven candidates based on calculation of the variation of turbulent friction factor constant as pin number increases from 19 to 61 as Appendix B shows. However, only two candidate sets can calculate increasing friction factor constants from 7 pin to 19 pin at H/D = 8 and P/D = 1.17.

These Table 3 results indicate that (-9,18) has a slightly better 90% confidence interval hence better pressure drop prediction than other sets. While set (-8,17) has the best flow split prediction, its performance like that of all other sets while inferior to the original CTD is still the same order as the measurement uncertainty.

Before selecting the W_{sT} set for adoption in the UCTD correlation, let us examine specifically the performance of W_{sT} (a,b) sets for the 19 pin bundle data now available to focus upon correction of the CTD reverse pin number effect. Recall the 19-pin bundle data, have been always over predicted by CTD due to its reversed pin number effect

There are nine 19-pin bundle data in the selected 80-bundle set and plus twenty-four Rehme 19-pin bundles of which only one was selected in the assessment of Chen et al.(2014). The pressure drop prediction results for these thirty-three bundles are presented in Table 4. It shows that our UCTD over predicts the 19-pin bundle friction factor results by about 3–5%, while existing CTD over predicts by about 10%. The result from this 19-pin bundle prediction set shows that (-11,19) has the smallest 90% confidence interval, hence the best performance.

If the pin number is decreased to 7, the indices for goodness of fit assessed by these W_{sT} using 20 Rehme's 7-pin bundles as data base are shown in Table 5. For the 7-pin bundle prediction the W_{sT}(-11,19) also has the smallest 90% confidence interval. This confirms that (-11,19) best represents the pin number effect. As well this W_{sT} set also predicts friction factor trends for pin bundle numbers greater than 7 up to 271.

For our three goals, the set (-11,19) has the best prediction regarding the pin number effect, set (-8,17) has the best prediction for flow split (see the last column in Table 3) and (-9,18) is somewhat better in predicting friction factor behavior for the 80-bundle data set (as illustrated by the 90% confidence level values in Table 3). Since the pressure drop predictions are similar to CTD, the set with best pin number effect, i.e., (-11,19) was selected for UCTD.

The empirical constants of W_{dT} for W_{sT} (-11,19) are fitted on a least square basis by a MATLAB program to be,

$$W_{dT} = \left(19.56 + 98.71\left(\frac{D_w}{D}\right) + 303.47\left(\frac{D_w}{D}\right)^2\right)\left(\frac{H}{D}\right)^{-0.541} \tag{14}$$

The turbulent bundle friction factor constants calculated using Eq. (14) to create UCTD for H/D = 12.5 and various P/D are compared with Rehme's data in Fig. 8.

This figure shows that the proposed W_{sT} set leads to correct prediction of the trend of C_{fbT} with increasing pin number as well as the magnitude of this parameter.

3.3.4. Empirical constants for the laminar regime W_{dL} and W_{sL}

Laminar region experimental constants were calibrated using the 23 bundle data set performed before 2014. The geometrical parameters and the laminar friction factor constants of these bundles are listed in Table B1 in Appendix B.

The laminar empirical constants W_{sL} and W_{dL} in CTD were assumed to be proportional to the turbulent constants. For W_{dL}, the coefficient can be derived theoretically to be approximately 1.4 (Cheng and Todreas, 1986). Given W_{dL}, (=1.4W_{dT}) and a preset coefficient for W_{sL}(=cW_{sT}), the bundle friction factor constant in the laminar regime for each of 23 bundles, can be predicted by the following formula (Cheng and Todreas, 1986),

$$C_{fbL} = De_b\left(\sum_{i=1}^{3}\left(\frac{N_iA_i}{A_b}\right)\left(\frac{De_i}{De_b}\right)\left(\frac{De_i}{C_{fiL}}\right)\right)^{-1} \tag{15}$$

In which

$$C_{f1L} = C'_{f1L}\left(\frac{P'_{w1}}{P_{w1}}\right) + W_{dL}\left(\frac{3A_{r1}}{A'_1}\right)\left(\frac{De_1}{H}\right)\left(\frac{De_1}{D_w}\right) \tag{16}$$

$$C_{f2L} = C'_{f2L}\left(1 + W_{sL}\left(\frac{A_{r2}}{A'_2}\right)\tan^2\theta\right) \tag{17}$$

$$C_{f3L} = C'_{f3L}\left(1 + W_{sL}\left(\frac{A_{r3}}{A'_3}\right)\tan^2\theta\right) \tag{18}$$

For the constant c above (i.e., cW_{sT}) a spectrum of values from 0.3 to 1.2 were selected, and the calculated C_{fbL} was compared with the data shown in Table B1. The calibrated value of c which gives the smallest 90% confidence interval is 1.0, as illustrated in Table 6. Hence the empirical constants for UCTD, the laminar wire drag and wire swirl constants were selected as,

$$W_{dL} = 1.4W_{dT} \tag{19}$$

$$W_{sL} = 1.0W_{sT} \tag{20}$$

3.4. Extending the capability in predicting 7-pin bundles

There are only twenty 7-pin bundles pressure drop experiments performed by Rehme (1967). The predictions of the original CTD were not applicable to 7-pin bundles due to the reversed pin number effect.

Table 3
Goodness of the pressure drop and edge subchannel flow split predictions of the seven candidate W_{sT} sets for the 80 bundle turbulent flow regime data.

Model\Index	Mean Error	STD of Error	90% C. I.	Mean RMS	Flow split error (X_2)
WsT (-8,17)	0.70%	8.03%	± 13.26%	6.40%	8.5%
WsT (-9,18)	1.34%	7.89%	± 13.16%	6.45%	8.8%
WsT (-10,18)	0.79%	8.23%	± 13.59%	6.57%	9.0%
WsT (-10,19)	0.73%	8.04%	± 13.28%	6.38%	8.6%
WsT (-11,19)	1.38%	8.12%	± 13.55%	6.63%	9.3%
WsT (-11,20)	1.36%	7.89%	± 13.17%	6.41%	9.3%
WsT (-12,21)	1.37%	7.89%	± 13.18%	6.39%	9.0%
Existing CTD	0.44%	7.96%	± 13.11%	7.03%	2.4%

Table 4
Goodness of prediction for 33 19-pin bundles for the turbulent regime data.

Model\Index	Mean Error	STD of Error	90% C. I.	Mean RMS
W_{sT} (-8,17)	3.37%	10.49%	± 18.13%	8.71%
W_{sT} (-9,18)	4.76%	9.64%	± 17.68%	8.33%
W_{sT} (-10,18)	2.82%	10.44%	± 17.79%	8.51%
W_{sT} (-10,19)	3.16%	10.56%	± 18.13%	8.71%
W_{sT} (-11,19)	4.07%	9.64%	± 17.21%	8.01%
W_{sT} (-11,20)	4.52%	9.71%	± 17.62%	8.25%
W_{sT} (-12,21)	4.39%	9.75%	± 17.59%	8.22%
Existing CTD	9.45%	8.73%	± 20.65%	11.08%

Table 5
Goodness of prediction for Rehme's twenty 7-pin bundles for the turbulent regime data.

Model\Index	Mean Error	STD of Error	90% C. I.	Mean RMS
W_{sT} (-8,17)	6.90%	15.36%	± 27.69%	14.58%
W_{sT} (-9,18)	10.98%	12.87%	± 27.57%	14.91%
W_{sT} (-10,18)	8.61%	13.68%	± 26.55%	14.24%
W_{sT} (-10,19)	6.44%	15.26%	± 27.25%	14.32%
W_{sT} (-11,19)	8.32%	13.67%	± 26.29%	14.08%
W_{sT} (-11,20)	10.42%	12.84%	± 27.00%	14.50%
W_{sT} (-12,21)	10.14%	12.84%	± 26.74%	14.32%
Existing CTD	26.08%	13.81%	± 43.78%	28.22%

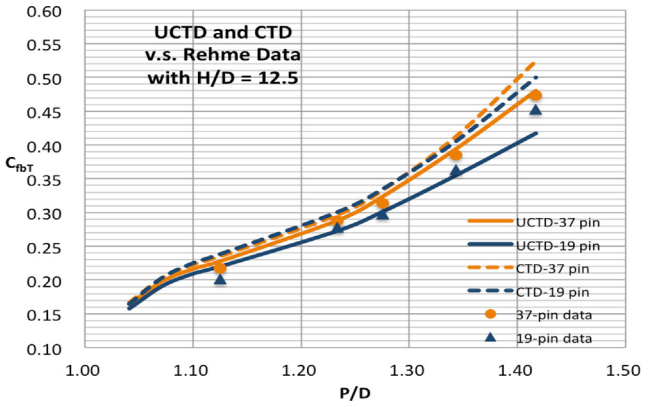

Fig. 8. Turbulent bundle average friction factor constant predicted by UCTD (-11,19) and CTD versus Rehme data with 37- and 19-pins for H/D = 12.5.

We hence have investigated the degree of CTD over prediction of the turbulent friction factor of the 7-pin bundle data, and whether UCTD would be able to solve this issue. Table 7 depicts the prediction error statistics for CTD, UCTD and REH for these twenty 7-pin bundles as well as that for the thirty-three 19-pin bundles. In general, CTD over predicts 7-pin results about 26%, while UCTD over predicts by only about one third of that amount or 9%, which is about the uncertainty of the data.

An expanded evaluation of UCTD predictions for 7-pin bundles evaluating the bundle friction factor variations over the interest range of the geometric parameters H/D and P/D is presented in Figs. 9a–9e. Specifically these figures show the turbulent constant predicted by UCTD compared with data for 7, 19 and 37 pin bundles as P/D varies given five H/D = 8.33, 12.5, 16.67, 25 and 50, respectively. The data

Table 7
Indices for goodness of correlation predictions of transition and turbulent data of 33 19-pin bundles and 20 7-pin bundles.

Model\Index	Mean Error	STD of Error	90% C. I.	Mean RMS
CTD-19 pin	6.48%	10.24%	± 19.91%	11.28%
CTD-7 pin	26.08%	13.81%	± 43.78%	28.22%
UCTD-19 pin	2.04%	9.31%	± 15.68%	8.21%
UCTD-7 pin	8.70%	13.59%	± 26.49%	14.21%
REH-19 pin	−4.48%	7.25%	± 14.01%	6.64%
REH-7 pin	−2.64%	5.22%	± 9.62%	5.33%

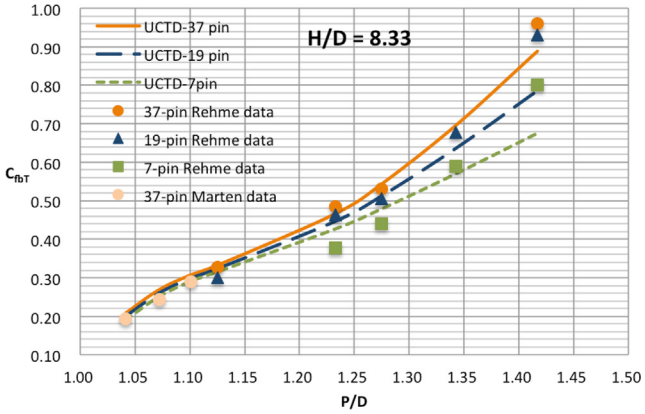

Fig. 9a. Turbulent bundle average friction factor constant predicted by UCTD (-11,19) versus Rehme and other data with 37- 19- and 7-pins for H/D = 8.33.

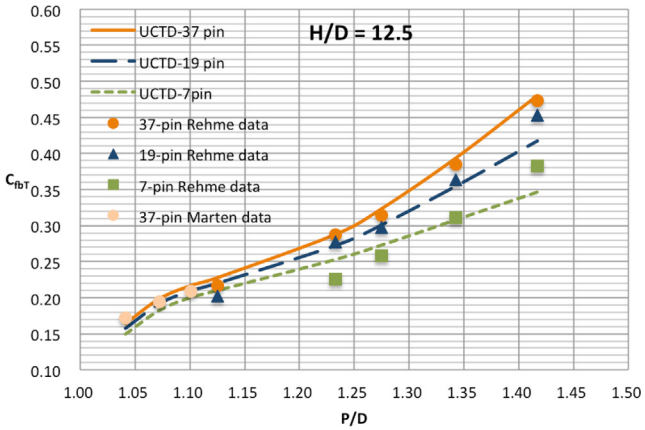

Fig. 9b. Turbulent bundle average friction factor constant predicted by UCTD (-11,19) versus Rehme and other data with 37- 19- and 7-pins for H/D = 12.5.

shown by other investigators has been taken from cases of H/D values near but not exactly equal to the five H/D values above representative of Rehme's bundles. The values presented in these figures have been adjusted by the difference predicted by UCTD.

As it can be seen from Figs. 9a–9c the predictions for 7-pin bundles with H/D lower than 17 are quite good. The discrepancy between prediction and data of 7 pin bundles mainly occurs at H/D = 25 and 50 as shown in Figs. 9d and 9e. In these two figures, it shows that Rehme's data for high H/

Table 6
Goodness of laminar constant Predictions for fractional W_{sL} values with fixed W_{sT} (-11,19).

W_{sL} =	$0.7W_{sT}$	$0.8W_{sT}$	$0.9W_{sT}$	$1.0W_{sT}$	$1.1W_{sT}$	$1.2W_{sT}$
Mean Error	−3.19%	−2.66%	−2.13%	−1.62%	−1.12%	−0.63%
STD of Error	11.89%	11.89%	11.93%	11.99%	12.07%	12.17%
90% C.I.	± 20.25%	± 20.08%	± 19.96%	± 19.90%	± 19.94%	± 20.04%
RMS	12.06%	11.93%	11.86%	11.84%	11.86%	11.92%

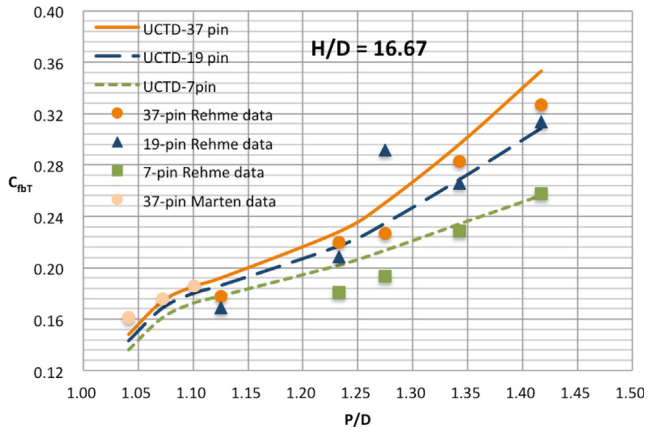

Fig. 9c. Turbulent bundle average friction factor constant predicted by UCTD (-11,19) versus Rehme and other data with 37- 19- and 7-pins for H/D = 16.67.

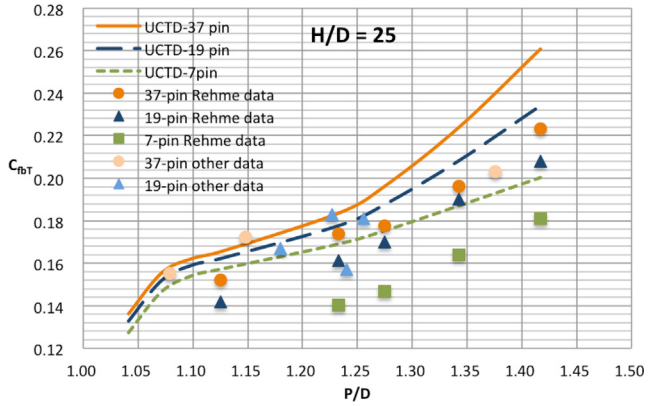

Fig. 9d. Turbulent bundle average friction factor constant predicted by UCTD (-11,19) versus Rehme and other data with 37- 19- and 7-pins for H/D = 25.

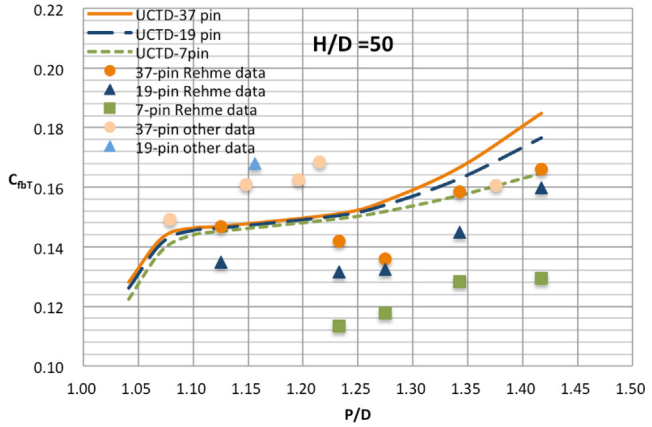

Fig. 9e. Turbulent bundle average friction factor constant predicted by UCTD (-11,19) versus Rehme and other data with 37- 19- and 7-pins for H/D = 50.

D are much lower than other investigators' results. Although there are no comparable 7-pin bundle data from other investigators, it is reasonable to expect that the data from Rehme are likely to be lower than the real values in the turbulent regime. This could cause the large over prediction of Rehme's 7-pin data. If the eight high H/D bundles are excluded from the data set, i.e., only twelve 7-pin bundles are in the data base, then the results, shown in the second column of Table 8, indicate that UCTD predicts 7-pin bundle results satisfactorily, with a mean error of 1.4% and a 90% confidence interval of ± 17.5%. The REH predicts this data set with similar accuracy to that of the previous twenty 7-pin bundle case.

Assuming UCTD is applicable to 7-pin bundles, then the total sodium fast reactor hexagonal wire wrapped type bundle experiments including 20 7-pin bundles becomes 138 (109 + 9 + 20) bundles. The statistic analysis results show that for UCTD the mean error for this complete data base for the transition and turbulent regimes is 2.2% with a 90% confidence interval of ± 17.3%. With this complete bundle data set, in which more than half were performed by Rehme (74 bundles), the REH has a mean error of -2.0% and a 90% confidence interval of ± 15.5%.

Finally, if the worst 7-pin high H/D bundles results, which are suspected to be too low, were excluded from the data base, the bundle number becomes 130 (138-8). The performance of UCTD improves dramatically, with a mean error of 1.1%, a 90% confidence interval of ± 15.3%. These results are better than REH's performance. Table 8 also shows explicitly in the last column the UCTD performance for the segregation of the 138 bundles by investigator i.e. non-Rheme and Rehme bundles.

From the above discussion, since the confidence interval for the 7 pin bundle predictions when excluding the 8 high H/D Rehme bundles is about the same as the confidence interval for all the other bundles combined, it is considered that UCTD is applicable to 7-pin bundles.

4. Discussion

4.1. Prediction accuracy of UCTD

The prediction capability of the proposed UCTD, will be examined in this section along with other correlations, the CTD, CTS, UCTS, and REH. The UCTD and UCTS formulations are presented in detail in Appendix A. The UCTS is CTS with the revised Re_{bL} value and transition equation presented in Sections 3.1 and 3.2, respectively. Two data bases are used to evaluate the goodness of correlation fit. The first is the 80-bundle data set used as the evaluation basis in the assessment of Chen et al. (2014). The results of indices for goodness of fit of these correlations are shown in Table 9 (upper value). According to these results, the order of performance based on 90% confidence interval is UCTD, CTD, UCTS, CTS and REH.

If a new data set is constructed from all the wire wrapped bundles with pin number higher than 7, i.e., including Rehme's 29 higher than 7-pin bundles which are excluded from the 80-bundle set plus 9 new bundles identified in Table 2, the total bundle number becomes 118 (80 + 29 + 9). Establishing these 118 bundles as the second data set, the indices for these correlations are also found in Table 9 (the lower values). The placement of REH in the order of goodness of predictions, based on 90% confidence interval, significantly improves, i.e., the order becomes UCTD, CTD&REH, UCTS and CTS. It can be concluded that for both data sets UCTD is better than all the other correlations. Fig. 10 compares the friction factor predicted by UCTD and the data for all 118 bundles in the transition and turbulent regimes. The prediction error distribution for this case is shown in Fig. 11. With this complete data set, as shown in Table 9 the UCTD has a prediction mean error of 0.95% and a standard deviation of 9.0% leading to a 90% confidence interval of ± 14.8%, while both REH and CTD have 1% and 1.5% higher values in the last two statistics parameters, i.e., STD and 90% confidence interval, respectively.

A specific analysis for the turbulent regime, based on the 118-bundle data set, the mean error, standard deviation, and 90% confidence interval for UCTD, CTD and REH are (2.4%, 2.9%, −3.8%), (8.2%, 9.1%, 7.6%) and (± 14.1%, ± 15.8%, ± 13.9%), respectively. As recognized by some investigators (Chun and Seo, 2001), REH tends to under predict the data. As for the laminar regime, out of 27 (23 + 4 new bundles) laminar data, UCTD is slightly better than CTD with mean and RMS values of (−2.0%, 9.5%) versus (−3.0%, 9.6%).

Finally, the prediction capability of UCTD to those nine recent experiments described in Table 1 were investigated for the validation of UCTD. There are in total 125 data points from these experiments; the

Table 8
Indices for goodness of correlation predictions of transition and turbulent data of different bundles sets.

Index \Data Set		Twenty 7-pin bundles	Twelve 7-pin bundles	All 138 bundles	All 64 non Rehme bundles	All 74 Rehme bundles
CTD	Mean Error	26.08%	21.30%	5.83%	−1.39%	10.33%
	STD of Error	13.81%	14.92%	13.90%	9.22%	14.41%
	90% C.I.	± 43.78%	± 40.43%	± 24.99%	± 15.35%	± 29.06%
UCTD	Mean Error	8.70%	1.30%	2.21%	−0.60%	3.96%
	STD of Error	13.59%	10.56%	10.27%	9.04%	10.59%
	90% C.I.	± 26.49%	± 17.50%	± 17.28%	± 14.90%	± 18.61%
REH	Mean Error	−2.64%	−2.51%	−1.99%	−1.72%	−2.16%
	STD of Error	5.22%	5.24%	9.22%	13.15%	5.49%
	90% C.I.	± 9.62%	± 9.56%	± 15.51%	± 21.82%	± 9.71%

Table 9
Indices for goodness of correlation predictions of transition and turbulent data of 80- and all 118-bundle.

Index	Model				
	CTD	UCTD	CTS	UCTS	REH
Mean[a]	−0.37%	0.34%	1.69%	1.31%	−1.45%
Error	1.91%	0.95%	3.25%	2.77%	−1.86%
STD of Error	9.35%	8.98%	11.24%	10.66%	11.46%
	9.94%	8.97%	10.89%	10.37%	9.80%
90% C. I.	± 15.39%	± 14.78%	± 18.69%	± 17.66%	± 19.01%
	± 16.64%	± 14.84%	± 18.70%	± 17.66%	± 16.41%
Mean RMS	8.30%	7.58%	10.23%	9.46%	8.62%
	9.01%	7.72%	10.27%	9.56%	7.71%

[a] Upper values for 80 bundle data set; lower values for the 118 bundle data set.

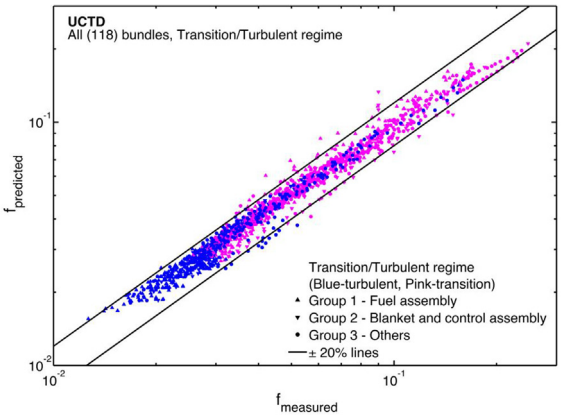

Note: Fuel assembly: P/D:1.1-1.3; H/D:20-54; Blanket and control assembly: P/D:1.03-1.13; H/D:7-23.

Fig. 10. Comparison of predictions by the Upgraded CTD to the measured friction factor of all 118 bundles in the transition and turbulent regimes.

mean, STD and 90% C.I. of prediction errors for UCTD, CTD and REH are (1.6%, −1.4%, −0.8%), (6.3%, 7.7%, 6.8%) and (± 10.7%, ± 12.8%, ± 11.2%), respectively. Also the averaged RMS for prediction errors of these correlations are (6.8%, 7.8%, 7.2%), and every bundle is predicted with an averaged RMS less than 10% by UCTD.

4.2. Prediction status for different H/D and P/D ranges

To check whether there is an imbalance in prediction of bundle groups of different geometry ranges, the 80-bundle data set is first separated into two groups based on their H/D values. The criteria is set at H/D = 20; those bundles with H/D < 20 are assigned to the small H/D group, and the others to the large H/D group. There are 34 bundles in the small H/D group, and 46 bundles in the large H/D group. The

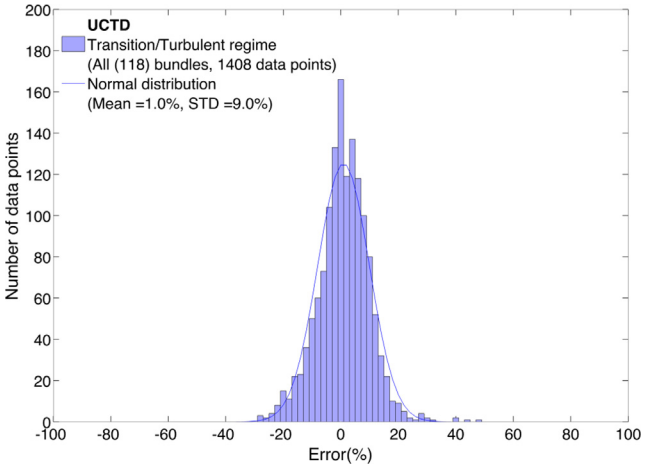

Fig. 11. Prediction error histogram for the Upgraded CTD for all 118 bundles in the transition and turbulent regimes.

prediction indices for these two groups are compared in Table 10. For the Mean Error, UCTD under predicts the small H/D group by 1.1%, and over predicts the large H/D group by 1.4%. For the key index of 90% confidence interval the UCTD results are about 15% and the most balanced. It is worth noticing that REH under predicts high H/D bundles about 4% (mean error), and has a large standard deviation for small H/D bundles.

For predictions for different P/D ranges, the group separation value is taken as 1.18. There are 32 bundles with P/D < 1.18 and 48 bundles with P/D ≧ 1.18 in the 80 bundle data set. Table 11 illustrates the prediction status for these two groups among five correlations. It can be seen that CTD and UCTD both predict these two groups in a very balanced and accurate manner, while the REH predicts small P/D bundles poorly (90% C.I.). It is concluded that UCTD produces good balanced predictions in both H/D and P/D ranges.

Table 10
Comparison of the prediction statistics for small H/D (< 20) and large H/D (≧ 20) bundles for 80 bundle data set in the transition and turbulent regimes.

Index	Model				
	CTD	UCTD	CTS	UCTS	REH
Mean[a]	−0.6%	−1.2%	1.0%	0.8%	1.5%
Error	−0.2%	1.6%	2.3%	1.8%	−3.9%
STD of Error	9.6%	8.9%	11.8%	11.0%	13.5%
	9.1%	8.9%	10.7%	10.4%	8.8%
90% C. I.	± 15.9%	± 14.7%	± 19.5%	± 18.1%	± 22.3%
	± 15.0%	± 14.9%	± 18.0%	± 17.3%	± 15.8%
Mean RMS	8.7%	8.1%	11.2%	10.4%	9.2%
	8.0%	7.2%	9.5%	8.8%	8.2%

[a] Upper value for low H/D group, lower value for high H/D group.

Table 11
Comparison of the prediction statistics for low P/D (< 1.18) and high P/D (≧ 1.18) bundles for 80 bundle data set in the transition and turbulent regimes.

Index	Model				
	CTD	UCTD	CTS	UCTS	REH
Mean[a] Error	−0.9%	−1.2%	−2.2%	−3.2%	0.6%
	0.0%	1.4%	4.1%	4.2%	−2.8%
STD of Error	9.4%	8.9%	10.3%	10.1%	14.7%
	9.3%	9.0%	11.1%	10.0%	8.5%
90% C. I.	± 15.5%	± 14.7%	± 17.4%	± 17.4%	± 24.2%
	± 15.3%	± 14.8%	± 19.5%	± 17.9%	± 14.8%
Mean RMS	8.6%	7.9%	9.7%	9.6%	10.5%
	8.1%	7.4%	10.5%	9.4%	7.3%

[a] Upper value for low P/D group, lower value for high P/D group.

4.3. Comparison between UCTD predictions new specific bundle experiments

Six sets of bundle data are of interest because of their differing pin numbers with identical geometry (THEADES and COMPLOT), the prior unsatisfactory prediction by CTD (ESTHAIR) and the current shortcoming in their prediction by UCTD (PGSFR2), in addition to the most recent one performed in USA (TAMU). An evaluation of these several sets compared to the UCTD is presented here. All other bundle sets of Table 1 are reasonably well predicted by UCTD.

The two experiments, THEADES (19 pin bundle) and COMPLOT (127 pin bundle) are most relevant in evaluating the predictive performance of UCTD which has been specifically formulated to predict the effect of pin number differences, since they have the same geometrical parameters but different pin numbers. Fig. 12 illustrates that the UCTD predicts the data of both bundles well, The trend of the pin number effect is now confirmed to be as it has been modeled by UCTD. The statement claimed in the original publication (Pacio et al., 2017) that CTD predicted the data unsatisfactory is not consistent with our calculations, which show that CTD under predicts about 6% in the turbulent regime.

The bundle, ESTHAIR, investigated by Berthoux and Cadiou (2010) used air as the working fluid. The CTD could not predict its data satisfactorily as reported by Chen et al. (2014). Fig. 13 shows the performance of the UCTD, CTD and REH relative to prediction of the ESTHAIR bundle friction factor data. This data can be well predicted by REH. The CTD over predicts the friction factor results about 18%, while UCTD reduces this over prediction to around 10% due to the correction of the pin number effect. However, this conclusion does not apply to the last data point, which deviates suddenly from the trend and was over predicted 25% and 18% by CTD and UCTD, respectively. For data to be predicted outside two standard deviations (SDV for UCTD in the turbulent regime = 8.1%) is unlikely, since the probability of this to happen is about 2%. (Note that the probability that the sample point will be outside two standard deviation for a normal distribution is 2.3%).

Two PGSFR bundles were tested. For the PGSFR1 (37-pin) bundle the CTD and UCTD predict data accurately, but REH under predicts the data around 14%. For PGSFR2, the REH predicts the data accurately while UCTD over predicts by about 10%. Since the geometrical parameters for these two bundles are almost identical (same P/D = 1.125, for 37-pin H/D = 27.69; 61-pin H/D = 29.86), the 10% difference between prediction and experiment for each of UCTD and REH implies to us that the data from at least one of the bundles are off from the real value. Hence this discrepancy is left to the experimenters to reevaluate their reported data.

As for the TAMU results, the data remeasured by rods with regular roughness replacing the extremely smooth acrylic rods (Veghetto et al., 2018); the numerical values were provided by Professor Hassan (2018) are compared with prediction of UCTD, CTD and REH in Fig. 14. The results show that the data in the laminar and turbulent regimes are well predicted, including the two transition boundaries. In the transition regime UCDT slightly over predicts the data.

5. Conclusions

This study has improved the prediction performance ability of the CTD by developing enhanced equations and constants for reformulation of the CTD correlation thereby creating the Upgraded CTD (UCTD) correlation. These enhancements, summarized below, have been developed based on the availability of new bundle data published over the last decade principally in the laminar and transition flow regimes as summarized in Section 1.3 of this paper.

a) A more realistic laminar to transition boundary as a function of P/D. The Re_{bL} value has been recalibrated to a smaller value shown in Eq. (3) which dramatically improves the prediction performance near the laminar boundary for transition regime values.
b) A revised equation for calculating the transition friction factor, as shown in Eq. (4), which gives a smooth friction factor curve from the transition to the turbulent regime. The work in this study proposes revision of the constant λ from 13 to 7.
c) Revised wire related empirical constants, wire drag constant (W_d) and wire swirl constant (W_s) to correct the effect of pin number on pressure drop prediction and as well yield better overall correlation prediction performance. The four empirical constants, wire drag constant and wire sweeping constant, for the turbulent and laminar regimes, in CTD have been revised to,

$$W_{sT} = -11.0\log\left(\frac{H}{D}\right) + 19.0 \tag{21}$$

$$W_{dT} = \left(19.56 + 98.71\left(\frac{D_w}{D}\right) + 303.47\left(\frac{D_w}{D}\right)^2\right)\left(\frac{H}{D}\right)^{-0.541} \tag{22}$$

$$W_{dL} = 1.4W_{dT} \tag{23}$$

$$W_{sL} = 1.0W_{sT} \tag{24}$$

Implementation of these revisions into CTD yields an updated correlation designated as upgraded CTD (UCTD). For the geometrical parameters of P/D up to 1.42 and H/D between 8 and 52, the pin number effect had been confirmed to be correct. The UCTD 90% prediction confidence interval for available 118 bundles (excluding 7 pin bundles) for turbulent and transition regimes is ± 14.8%, while for the CTD it is ± 16.6%. However, the predicted flow split for the edge subchannel is about 9% higher than the data, which is within the experimental uncertainty of the measured flow split values summarized in Table B4.

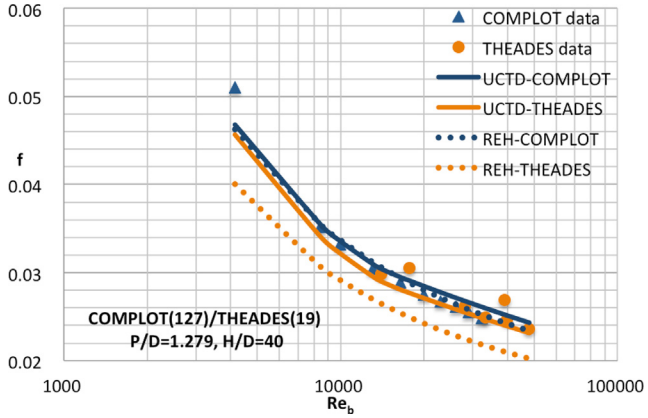

Fig. 12. Comparisons between THEADES and COMPLOT bundles data and predictions by UCTD and REH.

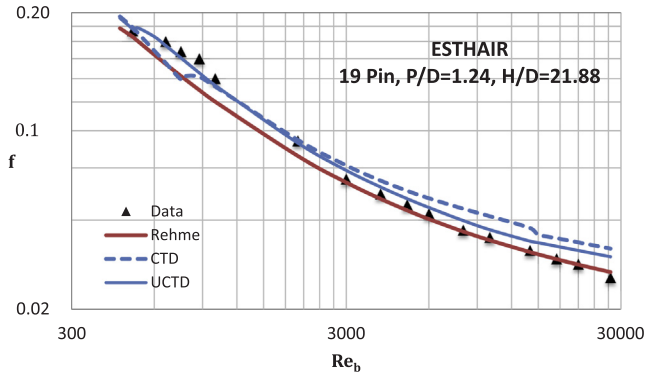

Fig. 13. The predictions of REH, CTD and UCTD compared to the ESTHAIR bundle friction factor data.

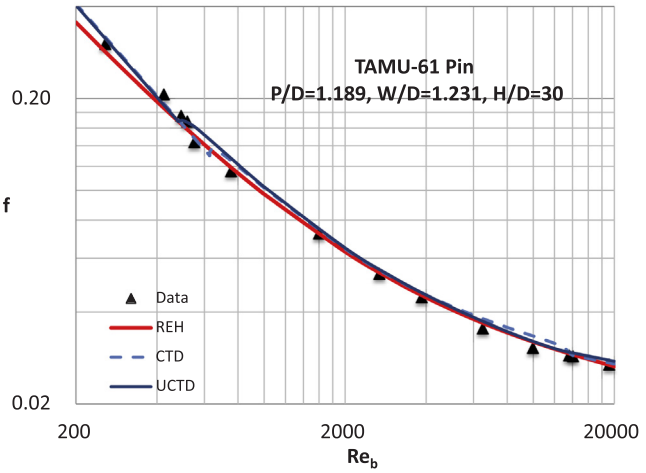

Fig. 14. Comparison between TAMU results (new data provided by Professor Hassan (2018)) and predictions of UCTD.

d) The UCTD is now applicable to 7 pin bundles. The mean error prediction for 7-pin bundles by UCTD is 9%, which is about the measurement uncertainty and an improvement from 26% with CTD.

Acknowledgements

The authors acknowledge Uchenna Oparaji, being an exchange student from Liverpool University to Tsing-Hua University, Taiwan, for writing a MATLAB program for fitting the wire drag constants. Thanks are given to MIT student Andres Alvaraz, for discussing how to solve a relevant nonlinear equation and providing a MATLAB program to find the solution. In addition the regression and fitting method suggested by MIT student, Ravikishore Kommajosyula and his advisor, Professor Emilio Baglietto, are highly appreciated. Recognition is also extended to Dr. Syeilendra Pramuditya for his updated code reflecting the upgraded CTD on the web. Most recently, the raw data of the TAMU bundle experiment has been provided by Professor Hassan of Texas A& M University which we greatly appreciate.

Appendix A: Upgraded Cheng and Todreas correlation

For laminar region, $Re_b < Re_{bL}$

$$f_i = \frac{C_{fiL}}{Re_i} \tag{A1}$$

For turbulent region, $Re_b > Re_{bT}$

$$f_i = \frac{C_{fiT}}{Re_i^{0.18}} \tag{A2}$$

For transition region, $Re_{bL} \leqq Re_b \leqq Re_{bT}$[5]

$$*f_i = \left(\frac{C_{fiL}}{Re_i}\right)(1-\psi_i)^{\frac{1}{3}}(1-\psi_i^7) + \left(\frac{C_{fiT}}{Re_i^{0.18}}\right)\psi_i^{\frac{1}{3}} \tag{A3}$$

where i = b, 1, 2 or 3 for bundle average, interior, edge and corner subchannel

$$*Re_{bL} = 320\left(10^{\left(\frac{P}{D}-1.0\right)}\right) \tag{A4}$$

$$Re_{bT} = 10{,}000\left(10^{0.7\left(\frac{P}{D}-1.0\right)}\right) \tag{A5}$$

$$\psi_i = \log\left(\frac{Re_i}{Re_{iL}}\right)/\log\left(\frac{Re_{iT}}{Re_{iL}}\right) \tag{A6}$$

For the detailed model (UCTD):

$$C_{fbL} = De_b\left(\sum_{i=1}^{3}\left(\frac{N_iA_i}{A_b}\right)\left(\frac{De_i}{De_b}\right)\left(\frac{De_i}{C_{fiL}}\right)\right)^{-1} \tag{A7}$$

$$C_{fbT} = De_b\left(\sum_{i=1}^{3}\left(\frac{N_iA_i}{A_b}\right)\left(\frac{De_i}{De_b}\right)^{0.0989}\left(\frac{De_i}{C_{fiT}}\right)^{0.54945}\right)^{-1.82} \tag{A8}$$

In which

[5] The equations with * are revised from CTD based on this study.

Table A1
Coefficients in Eq. (A19) for bare rod subchannel friction factor constants in hexagonal array.

Constant	1.0 ≦ P/D(W/D) ≦ 1.1			1.1 ≦P/D(W/D) ≦ 1.5		
	a	B	c	a	b	C
C_{f1L}'	26.00	888.2	−3334.0	62.97	216.9	−190.2
C_{f2L}'	26.18	554.5	−1480.0	44.40	256.7	−267.6
C_{f3L}'	26.98	1636.0	−10050.0	87.26	38.59	−55.12
C_{f1T}'	0.09378	1.398	−8.664	0.1458	0.03632	−0.03333
C_{f2T}'	0.09377	0.8732	−3.341	0.1430	0.04199	−0.04428
C_{f3T}'	0.1004	1.625	−11.85	0.1499	0.006706	−0.009567

$$C_{f1T} = C'_{f1T}\left(\frac{P'_{w1}}{P_{w1}}\right) + W_{dT}\left(\frac{3A_{r1}}{A'_1}\right)\left(\frac{De_1}{H}\right)\left(\frac{De_1}{D_w}\right)^{0.18} \tag{A9}$$

$$*W_{dT} = \left(19.56 + 98.71\left(\frac{D_w}{D}\right) + 303.47\left(\frac{D_w}{D}\right)^2\right)\left(\frac{H}{D}\right)^{-0.541} \tag{A10}$$

$$C_{f2T} = C'_{f2T}\left(1 + W_{sT}\left(\frac{A_{r2}}{A'_2}\right)\tan^2\theta\right)^{1.41} \tag{A11}$$

$$C_{f3T} = C'_{f3T}\left(1 + W_{sT}\left(\frac{A_{r3}}{A'_3}\right)\tan^2\theta\right)^{1.41} \tag{A12}$$

$$*W_{sT} = -11.0\log\left(\frac{H}{D}\right) + 19.0 \tag{A13}$$

$$C_{f1L} = C'_{f1L}\left(\frac{P'_{w1}}{P_{w1}}\right) + W_{dL}\left(\frac{3A_{r1}}{A'_1}\right)\left(\frac{De_1}{H}\right)\left(\frac{De_1}{D_w}\right) \tag{A14}$$

$$W_{dL} = 1.4W_{dT} \tag{A15}$$

$$C_{f2L} = C'_{f2L}\left(1 + W_{sL}\left(\frac{A_{r2}}{A'_2}\right)\tan^2\theta\right) \tag{A16}$$

$$C_{f3L} = C'_{f3L}\left(1 + W_{sL}\left(\frac{A_{r3}}{A'_3}\right)\tan^2\theta\right) \tag{A17}$$

$$*W_{sL} = 1.0W_{sT} \tag{A18}$$

Bare rod subchannel friction factor constants

$$C'_{fi} = a + b\left(\frac{P}{D}-1\right) + c\left(\frac{P}{D}-1\right)^2 \tag{A19}$$

For i = 1; for i = 2, 3 replace P/D by W/D (Table A1)
For the simplified model (UCTS)

$$C_{fbL} = \left(-974.6 + 1612.0\left(\frac{P}{D}\right) - 598.5\left(\frac{P}{D}\right)^2\right)\left(\frac{H}{D}\right)^{0.06-0.085\left(\frac{P}{D}\right)} \tag{A20}$$

$$C_{fbT} = \left(0.8063 - 0.9022\log\left(\frac{H}{D}\right) + 0.3526\left(\log\left(\frac{H}{D}\right)\right)^2\right)\left(\frac{P}{D}\right)^{9.7}\left(\frac{H}{D}\right)^{1.78-2.0\left(\frac{P}{D}\right)} \tag{A21}$$

The application ranges for UCTD are:

$7 \leqq N_r \leqq 271$
$1.0 \leqq P/D \leqq 1.42$
$8.0 \leqq H/D \leqq 52.0$

The application ranges for UCTS are:

$19 \leqq N_r \leqq 217$
$1.025 \leqq P/D \leqq 1.42$
$8.0 \leqq H/D \leqq 50.0$

Equations for geometrical parameters

A.1. Bare rod flow area and wetted perimeter

$$A_1' = (\frac{\sqrt{3}}{4})P^2 - \frac{\pi D^2}{8}$$

$$A_2' = P(W - \frac{D}{2}) - \frac{\pi D^2}{8}$$

$$A_3' = \frac{(W - \frac{D}{2})^2}{\sqrt{3}} - \frac{\pi D^2}{24}$$

$$A_b' = N_1 A_1' + N_2 A_2' + N_3 A_3'$$

$$P_{w1}' = \frac{\pi D}{2}$$

$$P_{w2}' = P + \frac{\pi D}{2}$$

$$P_{w3}' = \frac{\pi D}{6} + \frac{2\left(W - \frac{D}{2}\right)}{\sqrt{3}}$$

$$P_{wb}' = N_1 P_{w1}' + N_2 P_{w2}' + N_3 P_{w3}'$$

A.2. Wire-wrapped flow area and wetted perimeter

$$A_1 = A_1' - \frac{\pi D_w^2}{8\cos\theta}$$

$$A_2 = A_2' - \frac{\pi D_w^2}{8\cos\theta}$$

$$A_3 = A_3' - \frac{\pi D_w^2}{24\cos\theta}$$

$$A_b = N_1 A_1 + N_2 A_2 + N_3 A_3$$

$$P_{w1} = P_{w1}' + \frac{\pi D_w}{2\cos\theta}$$

$$P_{w2} = P_{w2}' + \frac{\pi D_w}{2\cos\theta}$$

$$P_{w3} = P_{w3}' + \frac{\pi D_w}{6\cos\theta}$$

$$P_{wb} = N_1 Pw1 + N_2 Pw2 + N_3 P_{w3}$$

Where $\cos\theta = \frac{H}{\sqrt{H^2 + (\pi(D + D_w))^2}}$

.

A.3. Wire projected area

$$A_{r1} = \pi(D + D_w)\frac{D_w}{6}$$

$$A_{r2} = \pi(D + D_w)\frac{D_w}{4}$$

$$A_{r3} = \pi(D + D_w)\frac{D_w}{6}$$

A.4. Hydraulic equivalent diameter

$$De_i' = \frac{4A_i'}{P_{wi}'}$$

$$De_i = \frac{4A_i}{P_{wi}}$$

where i = 1, 2, 3 or b

Appendix B: Process for determining empirical constants for the correct pin number effect

B.1. Description of the process

The new process employed was to guess a W_{sT} (expressed as Eq. (11), i.e., a*log(H/D)+b), then find the W_{dT} for each of the 80 bundles based upon the data of bundle average friction factor constant in the turbulent regime (determined by the average of the data of bundle friction factors multiplied by $Re_b^{0.18}$ in the turbulent regime). This 80 bundle geometrical information and associated turbulent constants are shown in Table B1. The W_{dT} for each bundle was calculated from Eq. (12) based upon equal pressure drop along the same bundle length for each type subchannel which relates the bundle average friction factor constant to the three subchannel friction factor constants and the number of each type subchannel

$$C_{fbT} = De_b\left(\sum_{i=1}^{3}\left(\frac{N_i A_i}{A_b}\right)\left(\frac{De_i}{De_b}\right)^{0.0989}\left(\frac{De_i}{C_{fiT}}\right)^{0.54945}\right)^{-1.82} \tag{12}$$

A W_{dT} equation with the form of

$$W_{dT} = \left(C_1 + C_2\left(\frac{D_w}{D}\right) + C_3\left(\frac{D_w}{D}\right)^2\right)\left(\frac{H}{D}\right)^{C_4} \tag{13}$$

was then calibrated by these 79 calculated W_{dT} values (one of the 80 bundles only has laminar data) to get the four constants of Eq. (13) (see Section 3.3.2 2nd paragraph).

To yield the correct pin number effect i.e. variation of bundle average friction factor as pin number changes, the edge subchannel friction factor should be smaller than that of the interior subchannel as discussed in Section 3.3.2. Apparently the W_{sT} value should be reversed from that of the original CTD, Eq. (8) as H/D increases. Testing of the different coefficients for this formulation of W_{sT} showed that only 7 sets of the constants a and b of Eq. (10) can give the correct pin number effect for H/D between 8 and 52 and P/D between 1.0 and 1.42, for pin number ≧ 19, as illustrated in Table B2. Out of these seven sets only two of them satisfy pin number effect from 7-pin to 19-pin.

B.2. Evaluation of the results of the process

The best (a,b) set of Eq. (10) should achieve the following results- 1) predict the correct pin number trend, 2) predict the friction factor data well and 3) predict the flow split consistent with data. To find out which set (a,b) can achieve the above 3 goals, a thorough study has been performed.

B.2.1. Pin number effect results

The pin number effect is correct based on the study of calculating the variation of turbulent friction factor constant as pin number increases from 7 to 61, and then to 217, over the range of H/D and P/D geometrical conditions of interest. The specific geometric conditions selected for checking the pin number effect are seven H/D (8.0, 8.33, 12.5, 16.67, 25, 50 and 52) coupled with sixteen P/D values (1.041, 1.072, 1.101, 1.125, 1.15, 1.16, 1.17, 1.18, 1.19, 1.20, 1.21, 1.22, 1.233. 1.275, 1.343 and 1.417). The reason for selecting these values is that the worst conditions for the reverse trend to occur are around H/D = 52 and P/D = 1.19 as well as H/D = 8 and P/D = 1.17 as known from a supplemental study. Based on study of this paper only 7 sets [(-8,17), (-9,18), (-10,18), (-10,19), (-11,19), (-11,20) and (-12,21)] of these constants listed in Table B2 can meet the pin number effect goal for pin number ≧ 19, and out of them only two [(-10,18) and (-11,19)] can predict the correct pin number trend for 7–19 pin bundles.

Each number in this table is (the higher pin number bundle friction factor constant − that of lower pin number bundle)/(lower pin number bundle friction factor constant). If all these values are positive at these worst geometrical conditions, then the pin number effect is correct. From Table B2 the following can be concluded,

a) only 7 sets [(-8,17), (-9,18), (-10,18), (-10,19), (-11,19), (-11,20) and (-12,21)] of these constants listed in Table B2 can meet the pin number effect goal for pin number ≧ 19, and
b) out of them only two [(-10,18) and (-11,19)] can predict the correct pin number trend for all pin number ≧ 7 bundles. Since the bundle friction factor from 7 to 19 pin is increasing at any geometrical condition.

B.2.2. Prediction of bundle friction factor

After fitting for W_{dT} through a MATLAB program using the form of Eq.(10) and inserting the new values for the two empirical constants, W_{dT} and $W_{sT,}$ into CTD. the C_{fbT} for each bundle was predicted. Using the prediction error of the 80 bundles data set in the turbulent regime to fit a normal distribution to get the mean (m) and standard deviation (σ) for each set of empirical constants, the results shown in Table B3 are obtained .

B.2.3. Prediction of flow split in the turbulent flow regime

Out of more than ten flow split experiments, eight of them are considered to be useful, including one recently published by Chang et al. (2016). The reason for taking out some results were that either the data of edge subchannel flow split were for the transition (versus the turbulent) regime or were less than 1.0, which is theoretically not possible. These data are listed in Table B4. Using the sets of W_{sT} and W_{dT} the flow split of X_2 for each bundle can be predicted.

The predictions of X_2 by seven candidates for the UCTD are listed in Table B5. However, all of them over predict the X_2 about 9% (see the last row in Table B5), which is considered within the measurement uncertainty. Hence the seven sets for W_{sT} coefficients all meet the three requirements as discussed above. These sets will be the seven candidates for the final selection process presented in the main text.

Table B1
Bundle geometrical parameters and average friction factor constants in the turbulent and laminar regimes for the 80 bundle data base.

ID[b,c]	Year	Pin	D (mm)	D_w (mm)	P/D	W/D	H/D	C_{fbT}	C_{fbL}
Marten11	1982	37	15.98	0.66	1.041	1.041	8.38	0.1925	45
Marten12	1982	37	15.98	0.66	1.041	1.041	12.6	0.1717	45
Marten13	1982	37	15.98	0.66	1.041	1.041	17.01	0.1602	45
Carelli	1981	61	12.7	0.635	1.05	1.05	20.0	0.1711	60
Chiu1	1979	61	12.73	0.8	1.067	1.069	8.0	0.2402	90
Marten21	1982	37	15.51	1.12	1.072	1.072	8.34	0.2427	68
Marten22	1982	37	15.51	1.12	1.072	1.072	12.54	0.1939	56
Marten23	1982	37	15.51	1.12	1.072	1.072	16.68	0.1758	56
Reihman1	1969	37	6.756	0.406	1.079	1.1	22.56	0.1581	–
Reihman2	1969	37	6.756	0.406	1.079	1.1	45.11	0.1503	–
Engel	1979	61	12.85	0.94	1.082	1.08	7.78	0.271	99
Marten31	1982	37	15.11	1.53	1.101	1.101	8.31	0.2908	80
Marten32	1982	37	15.11	1.53	1.101	1.101	12.31	0.2115	74
Marten33	1982	37	15.11	1.53	1.101	1.101	16.61	0.1859	68
Rehme11d	1967	61	12	1.5	1.125	1.125	8.33	0.3294	–
Rehme12d	1967	61	12	1.5	1.125	1.125	12.5	0.2202	–
Rehme13d	1967	61	12	1.5	1.125	1.125	16.67	0.1811	–
Rehme14d	1967	61	12	1.5	1.125	1.125	25.0	0.1545	–
Rehme15d	1967	61	12	1.5	1.125	1.125	50.0	0.1392	–
Reihman10	1969	217	6.35	0.762	1.135	1.143	48.0	0.1595	–
Reihman3	1969	37	6.35	0.762	1.148	1.171	12.0	0.2283	–
Reihman4	1969	37	6.35	0.762	1.148	1.171	24.0	0.174	–
Reihman5	1969	37	6.35	0.762	1.148	1.171	48.0	0.1616	–
Reihman11	1969	37	7.62	0.914	1.15	1.178	40.0	0.1606	–
Cheng	1984	37	15.04	2.26	1.154	1.164	13.4	0.2001	94
Burns	1980	37	12.72	1.91	1.156	1.177	21.0	0.1502	85
Reihman12	1969	19	6.35	0.762	1.156	1.184	48.0	0.1685	–
Baumann1	1968	61	6	1	1.167	1.167	16.7	0.1958	–
Baumann2	1968	61	6	1	1.167	1.167	25.0	0.1645	–
Itoh5	1981	127	5.5	0.9	1.176	1.178	38.0	0.1592	73
Itoh6	1981	127	5.5	0.9	1.176	1.178	53.27	0.1431	–
Chun4	2001	19	8	1.4	1.178	1.18	37.5	0.1573	91
Chun3	2001	19	8	1.4	1.18	1.176	25.0	0.1669	79
Reihman6	1969	37	6.096	1.016	1.196	1.22	50.0	0.1624	–
Choi	2003	271	7.4	1.4	1.2	1.2	24.84	0.1832	–
Itoh7	1981	169	6.5	1.32	1.214	1.214	47.39	0.1578	77
Reihman7	1969	37	5.994	1.08	1.215	1.24	50.85	0.1682	–
Itoh1	1981	91	6.3	1.27	1.216	1.216	15.03	0.2385	–
Itoh2	1981	91	6.3	1.27	1.216	1.216	22.54	0.1823	–
Itoh3	1981	91	6.3	1.27	1.216	1.216	32.22	0.1709	–
Itoh4	1981	91	6.3	1.27	1.216	1.216	45.08	0.1562	–
Okamoto	1970	91	6.3	1.39	1.221	1.221	40.48	0.1727	–
Wakasugi	1971	91	6.3	1.2	1.221	1.221	14.29	0.2357	–
Wakasugi	1971	91	6.3	1.2	1.221	1.221	20.63	0.2013	–
Wakasugi	1971	91	6.3	1.2	1.221	1.221	30.16	0.1712	–
Wakasugi	1971	91	6.3	1.2	1.221	1.221	41.27	0.15	–
Baumann3	1968	19	6.62	1.5	1.227	1.227	15.1	0.2642	–
Baumann4	1968	19	6.62	1.5	1.227	1.227	22.7	0.1897	–
Rehme21c	1967	37	12	2.8	1.233	1.233	8.33	0.4845	–
Rehme22c	1967	37	12	2.8	1.233	1.233	12.5	0.2874	–
Rehme23c	1967	37	12	2.8	1.233	1.233	16.67	0.2201	–
Rehme24c	1967	37	12	2.8	1.233	1.233	25.0	0.1739	–
Rehme25c	1967	37	12	2.8	1.233	1.233	50.0	0.1418	–
ESTHAIR	2010	19	16	3.84	1.24	1.24	21.88	0.1658	87
Efithimiadis	1983	19	18.92	4.60	1.245	1.245	35.2	–[a]	82
Spencer	1980	217	5.84	1.42	1.252	1.242	51.74	0.16	84
Chun2	2001	19	8	2	1.255	1.268	37.5	0.1638	102
Chun1	2001	19	8	2	1.256	1.265	25.0	0.181	114
Rehme31c	1967	37	12	3.3	1.275	1.275	8.33	0.53	
Rehme32c	1967	37	12	3.3	1.275	1.275	12.5	0.3139	–
Rehme33c	1967	37	12	3.3	1.275	1.275	16.67	0.2268	–
Rehme34c	1967	37	12	3.3	1.275	1.275	25.0	0.1777	–
Rehme35c	1967	37	12	3.3	1.275	1.275	50.0	0.1359	–
Davidson	1971	217	6.39	1.808	1.283	1.283	48.0	0.1594	–
ISPRA	2011	19	8	2.4	1.3	1.3	18.75	0.2812	–[a]
Hoffmann1	1973	61	6	1.9	1.317	1.317	16.67	0.2641	–
Hoffmann2	1973	61	6	1.9	1.317	1.317	33.33	0.172	–
Hoffmann3	1973	61	6	1.9	1.317	1.317	50.0	0.16	–
Rehme41b	1967	19	12	4.1	1.343	1.343	8.33	0.6767	–
Rehme42c	1967	37	12	4.1	1.343	1.343	12.5	0.3852	–
Rehme43c	1967	37	12	4.1	1.343	1.343	16.67	0.2825	–
Rehme44c	1967	37	12	4.1	1.343	1.343	25.0	0.1962	–
Rehme45c	1967	37	12	4.1	1.343	1.343	50.0	0.1586	–
Reihman8	1969	37	6.35	2.012	1.376	1.434	24.0	0.2072	–

(*continued on next page*)

Table B1 (*continued*)

ID[b,c]	Year	Pin	D (mm)	D_w (mm)	P/D	W/D	H/D	C_{fbT}	C_{fbL}
Reihman9	1969	37	6.35	2.012	1.376	1.434	48.0	0.1624	–
Rehme51c	1967	37	12	5	1.417	1.417	8.33	0.9586	–
Rehme52c	1967	37	12	5	1.417	1.417	12.5	0.4735	–
Rehme53c	1967	37	12	5	1.417	1.417	16.67	0.3267	–
Rehme54c	1967	37	12	5	1.417	1.417	25.0	0.2233	–
Rehme55c	1967	37	12	5	1.417	1.417	50.0	0.166	–

[a] No data in this regime.
[b] See Chen et al. (2014) for citations of all bundles.
[c] Working fluid is water except for ETHAIR (air) and Hoffman (sodium).

Table B2
Empirical constants W_{sT} that give the correct pin number effect for pin number ≧ 19 or ≧ 7.

(a,b) For W_{sT}	Percentage of friction factor constant change for H/D = 8.0, P/D = 1.17			Percentage of friction factor constant change for H/D = 52.0, P/D = 1.19		
	7-19 Pin	19-37 Pin	37-61 Pin	7-19 Pin	19-37 Pin	37-61 Pin
(-8,17)	−0.14%	1.20%	1.15%	0.05%	0.01%	0.03%
(-9,18)	−0.30%	1.10%	1.08%	0.18%	0.08%	0.07%
(-10,18)	2.36%	2.78%	2.24%	0.17%	0.07%	0.05%
(-10,19)	−0.47%	1.00%	1.01%	0.30%	0.15%	0.12%
(-11,19)	2.17%	2.67%	2.16%	0.31%	0.15%	0.11%
(-11,20)	−0.61%	0.91%	0.95%	0.43%	0.24%	0.17%
(-12,21)	−0.76%	0.82%	0.89%	0.55%	0.30%	0.21%

Table B3
W_{sT}(a,b) and the fitted W_{dT} as well as the mean, standard deviation and 90% confidence interval of prediction error for each set of turbulent wire constants.

(a,b) For W_{sT}	Fitted $W_{dT} = (C_1 + C_2(D_w/D) + C_3(D_w/D)^2)(H/D)^C_4$				80 bundle data in turbulent regime predicted Error statistics		
	C_1	C_2	C_3	C_4	m	σ	90% C.I.
(-8,17)	15.79	−79.21	229.26	−0.474	0.70%	8.03%	± 13.26%
(-9,18)	15.23	−76.17	219.69	−0.458	1.34%	7.89%	± 13.16%
(-10,18)	20.43	−103.50	319.61	−0.560	0.79%	8.23%	± 13.59%
(-10,19)	14.71	−73.36	210.94	−0.443	0.73%	8.04%	± 13.28%
(-11,19)	19.56	−98.71	303.47	−0.541	1.38%	8.12%	± 13.55%
(-11,20)	14.23	−70.77	202.93	−0.428	1.36%	7.89%	± 13.17%
(-12,21)	13.78	−68.36	195.59	−0.414	1.37%	7.89%	± 13.18%
(20,-7)[a]	29.5	−140	401	−0.85	0.44%	7.96%	± 13.11%

[a] Existing CTD.

Table B4
Flow split data for edge subchannel in the turbulent regime.

Experimentor	H/D	P/D	W/D	Pins	D (mm)	D_w (mm)	Re_b	X_2
Symolon and Todreas (1981)	51.72	1.25	1.25	217	5.89	1.47	12,720	1.041
Bartholet (1976)	51.68	1.257	1.257	217	63.6	15.88	73,000	1.04
Pedersen et al. (1974)	48	1.21	1.21	91	6.35	1.27	20,000	1.03
Davidson (1971)	48	1.283	1.227	217	6.39	1.81	20,000	1.01
Ohtake et al. (1976)	34.8	1.19	1.19	37	31.6	6	14,000	1.048
Chang et al. (2016)	27.69	1.125	1.125	37	7.4	0.93	37,100	1.018
Cheng (1984)	13.4	1.154	1.164	37	15.04	2.26	26,300	1.042
Chiu et al. (1978)	8	1.067	1.069	61	12.73	0.8	14,680	1.21

Table B5
Predictions of edge subchannel flow split in the turbulent regime by seven UCTD candidates.

Bundle	X_2-Data	WsT (-8,17)	WsT (-9,18)	WsT (-10,18)	WsT (-10,19)	WsT (-11,19)	WsT (-11,20)	WsT (-12,21)
Symolon	1.041	1.133	1.12	1.13	1.13	1.13	1.14	1.14
Bartholet	1.040	1.11	1.12	1.12	1.12	1.12	1.13	1.13
Pederson	1.030	1.10	1.10	1.10	1.11	1.11	1.11	1.11
Davidson	1.010	1.08	1.08	1.09	1.09	1.09	1.09	1.09
Ohtake	1.048	1.11	1.12	1.12	1.12	1.12	1.12	1.12
Chang	1.018	1.13	1.14	1.14	1.14	1.14	1.14	1.14
Cheng	1.042	1.20	1.21	1.23	1.21	1.23	1.21	1.21
Chiu	1.210	1.25	1.25	1.28	1.25	1.28	1.24	1.24
Mean error		8.5%	8.8%	9.0%	8.6%	9.3%	9.3%	9.0%

References

Bartholet, T.G., 1976. 11:1 Scale Wire-Wrap Rod Bundle Air Flow Test, Side Subchannels. WARD-D-0129.

Baxi, C.B., Dalle Donne, M., 1981. Helium cooled systems, the gas cooled fast breeder reactor. In: Fenech, H. (Ed.), Heat Transfer and Fluid Flow in Nuclear Systems. Pergamon Press Inc., pp. 410–462.

Berthoux, M., Cadiou, T., 2010. The thermal hydraulics in a rod bundle representative of the start-up core of the ALLEGRO gas cooled fast reactor—experimental and numerical approaches. Nucl. Eng. Des. 240, 3372–3386.

Bubelis, E., Schikorr, M., 2008. Review and proposal for best fit of wire-wrapped fuel bundle friction factor and pressure drop predictions using various existing correlations. Nucl. Eng. Des. 238, 3299–3320.

Chang, S.K., Euh, D.J., Choi, H.S., Kim, H., Choi, S.R., Lee, H.Y., 2016. Flow distribution and pressure loss in subchannels of a wire-wrapped 37-pin rod bundle for a sodium-cooled fast reactor. Nucl. Eng. Technol. 48, 376–385.

Chang, S.K., Euh, D.J., Kim, S., Choi, H.S., Kim, H., Ko, Y.J., Choi, S.R., Lee, H.Y., 2017. Experimental study of the flow characteristics in an SFR type 61-pin rod bundle using iso-kinetic sampling method. Ann. Nucl. Energy 106, 160–169.

Chen, S.K., Petroski, R., Todreas, N.E., 2013. Numerical implementation of the Cheng and Todreas correlation for wire wrapped bundle friction factors-desirable improvements in the transition flow region. Nucl. Eng. Des. 263, 406–410.

Chen, S.K., Todreas, N.E., Nguyen, N.T., 2014. Evaluation of existing correlations for the prediction of pressure drop in wire-wrapped hexagonal array pin bundles. Nucl. Eng. Des. 267, 109–131.

Cheng, S.K., 1984. Constitutive Correlations for Wire-wrapped Sub-channel Analysis Under Forced and Mixed Convection Conditions (Ph.D. thesis). Nuclear Engineering Department, MIT.

Cheng, S.K., Todreas, N.E., 1986. Hydrodynamic models and correlations for bare and wire-wrapped hexagonal rod bundles—bundle friction factors, sub-channel friction factors and mixing parameters. Nucl. Eng. Des. 92, 227–251.

Chenu, A., Mikityuk, K., Chawl, R., 2011. Pressure drop modeling and comparisons with experiments for single- and two-phase sodium flow. Nucl. Eng. Des. 241, 3898–3909.

Chiu, C., Rohsenow, W.M., Todreas, N.E., 1978. Flow-Split Model for LMFBR Wire-Wrapped Assemblies. COO-2245-56TR, Rev. 1. MIT.

Choi, S.K., Choi, I.K., Nam, H.Y., Choi, J.H., Choi, H.K., 2003. Measurement of pressure drop in a full-scale fuel assembly of a liquid metal reactor. J. Press. Vessel Technol. 125, 233–238.

Chun, M.H., Seo, K.W., 2001. An experimental study and assessment of existing friction factor correlations for wire-wrapped fuel assemblies. Ann. Nucl. Energy 28, 1683–1695.

Conti, A., Gerschenfeld, A., Gorsse, Y., 2017. Numerical Analysis of Core Thermal-Hydraulic for Sodium-Cooled Fast Reactors. NURETH-16, Chicago, IL, August 30-September 4, 2015.

Davidson, C.R., 1971. Hydraulic Tests on the 217-Rod Full-Sized Wire-Wrapped Fuel Assembly. TR-095-211-006, Atomic International Supporting Document.

Hassan, Y.A., 2018. Personal Communication to S.K. Chen.

Hu, R., 2017. SAM Theory Manual. Nuclear Engineering Division, Argonne National Laboratory (2017) ANL/NE-17/4.

Kim, W.S., Kim, Y.G., Kim, Y.J., 2002. A subchannel analysis code MATRA-LMR for wire wrapped LMR subassembly. Ann. Nucl. Energy 29, 303–321.

Kirillov, P.L., Bobkov, V.P., Zhukov, A.V., Yuriev, Y.S., 2010. Handbook on Thermohydraulic Calculations in Nuclear Engineering. Thermohydraulic Processes in Nuclear Power Facilities. Energoatomizdat, Moscow vol. 1.

Larsen, R.J., Marx, M.L., 2012. An Introduction to Mathematical Statistics and its Applications. Prence Hall Inc., New Jersey.

Lodi, F., Grasso, G., Mattioli, D., Sumini, M., 2016. ANTEO+: a subchannel code for thermal-hydraulic analysis of liquid metal cooled systems. Nucl. Eng. Des. 306, 128–152.

Marten, K., Yonekawa, S., Hoffmann, H., 1982. Experimental investigation on pressure drop in tightly packed bundles with wire wrapped rods. IAHR Second International Specialists Meeting on Thermal-hydraulics in LMFBR Rod Bundles, Rome, September, 1982.

Novendstern, E.H., 1972. Turbulent flow pressure drop model for fuel rod assemblies utilizing a helical wire-wrap spacer system. Nucl. Eng. Des. 22, 19–27.

Ohshima, H., Imai, Y., 2017. Numerical Simulation Method of Thermal-hydraulics in Wire-wrapped Fuel Pin Bundle of Sodium-cooled Fast Reactor. IAEA-CN245-453, 2017.

Ohtake, T., Uruwashi, S., Takahashi, K., 1976. Velocity measurements in the subchannel of the wire-spaced subassembly. Nucl. Technol. 30.

Pacio, J., Daubner, M., Fellmoser, F., Litfin, K., Wetzel, T., 2016. Experimental study of heavy-liquid metal (LBE) flow and heat transfer along a hexagonal 19-rod bundle with wire spacers. Nucl. Eng. Des. 301, 111–127.

Pacio, J., Litfin, K., Wetzel, T., Kennedy, G., Tichelen, K.V., 2017. Thermal-hydraulic Experiments Supporting the MYRRHA Fuel Assembly. IAEA-CN245-283.

Padmakumar, G., Velusamy, K., Prasad, B.V.S.S., Rajan, K.K., 2017. Hydraulic characteristics of a fast reactor fuel subassembly: an experimental investigation. Ann. Nucl. Energy 102, 255–267.

Pedersen, D. R., Pierce, R. D., Wilson, R. E., Roop, C. J., 1974. Experimental Investigation of the Hydraulic Entrance Length and Subchannel Velocity Profiles in a 91-Element Wire-Wrapped Subassembly. ANL/RAS 74-5.

Qvist, S., Greenspan, E., 2016. The ADOPT code for automated fast reactor core design. Ann. Nucl. Energy 71, 23–36.

Rehme, K., 1967. Geometry-dependence of the Pressure Loss in Rod Bundles with Coiled Wire Spacers and Longitudinal Flow (Ph.D. dissertation). U. Karlsruhe, Germany.

Rehme, K., 1972. Pressure drop performance od rod bundles in hexagonal ar, rangements. Int. J. Heat Mass Transfer 15, 2499–2517.

Rehme, K., 1973. Pressure drop correlations for fuel element spacers. Nucl. Technol. 17, 15–23.

Rolfo, S., Peniguel, C., Guillaud, M., Laurence, D., 2012. Thermal–hydraulic study of a wire spacer fuel assembly. Nucl. Eng. Des. 243, 251–262.

Symolon, P.D., Todreas, N.E., 1981. Fluid Mixing Studies in a Hexagonal 217-pin Wire Wrapped Rod Bundle. DOE/ET/37240-84TR, MIT.

Tenchine, D., 2010. Some thermal hydraulic challenges in sodium cooled fast reactors. Nucl. Eng. Des. 240, 1195–1217.

Veghetto, A., Jones, P., Goth, N., Childs, M., Lee, S., Nguye, D.H., Hassan, Y.A., 2018. Pressure measurements in a wire-wrapped 61-pin hexagonal fuel bundle. J. Fluids Eng. 140, 031104-1–031104-9.

Yang, W.S., Yacout, A.M., 1995. Assessment of the SE2-ANL Code Using EBR-II Temperature Measurements. In: Proc. 7th International Meeting on Nuclear Reactor Thermal Hydraulics, Saratoga Springs, New York, September 10–15, 1995, Vol. 3, pp. 2394–2409.